Contrib Mineral Petrol (2008) 156:721–743
DOI 10.1007/s00410-008-0312-2

ORIGINAL PAPER

Genesis of intermediate igneous rocks at the end of the Sveconorwegian (Grenvillian) orogeny (S Norway) and their contribution to intracrustal differentiation

Jacqueline Vander Auwera · Michel Bogaerts · Olivier Bolle · John Longhi

Received: 7 January 2008 / Accepted: 21 May 2008 / Published online: 13 June 2008

Abstract Abundant ferroan, metaluminous granitoids (970–950 Ma) emplaced at the end of the Sveconorwegian collisional orogeny (1130–900 Ma) are dominated by intermediate to silicic compositions with rare mafic facies. Both 73% fractional crystallization of an amphibole-bearing gabbroic cumulate substracted from the parent mafic composition and 30% non-modal batch melting of an amphibolitic source equivalent in composition to the mafic facies produce a monzodioritic liquid with appropriate trace element composition. A better fit is obtained for the partial melting process. Both processes could have occurred simultaneously to produce mafic cumulates and restites. As there is no evidence for large volumes of dense mafic rocks in the Sveconorwegian upper crust, these dense mafic rocks were probably produced in the lower crust. Formation of these granitoids, thus, contributed to the vertical stratification of the Proterozoic continental crust and also to the transfer of water from the lower crust to the surface.

Keywords Modeling of magma differentiation · Proterozoic continental crust · Postcollisional magmatism · Sveconorwegian (Grenvillian) granitoids

Communicated by J.L.R. Touret.

J. Vander Auwera (✉) · M. Bogaerts · O. Bolle
UR Pétrologie et Géochimie endogènes (B20),
Université de Liège, 4000 Sart Tilman, Belgium
e-mail: jvdauwera@ulg.ac.be

O. Bolle
e-mail: olivier.bolle@ulg.ac.be

J. Longhi
Lamont-Doherty Earth Observatory, Palisades, NY 10964, USA
e-mail: longhi@ldeo.columbia.edu

Introduction

Anorthositic complexes and rapakivi or rapakivi-like granites [those lacking the typical rapakivi texture but with composition similar to the rapakivi granites (Haapala and Rämö 1992)] are major components of the Proterozoic continental crust (e.g. Ashwal 1993; Emslie 1985; Rämö and Haapala 1995). Unraveling their petrology and their possible sources are thus key to understanding the formation of the continental crust during this period. In the Sveconorwegian (Grenvillian) orogeny (1130–900 Ma), the postcollisional magmatism (970–930 Ma) was voluminous and made of two magmatic suites: the Rogaland Anorthosite Complex, an Anorthosite–Mangerite–Charnockite (AMC) suite, and a suite of hornblende- and biotite- bearing granitoids (HBG) having geochemical signatures comparable to those of rapakivi granites (Andersen et al. 2001; Bingen et al. 2005; Bogaerts et al. 2003a; Vander Auwera et al. 2001, 2003) (Fig. 1). The petrology and geochemistry of the Rogaland Anorthosite Complex have been extensively discussed in the literature; the petrogenesis is consistent with partial melting of a lower crustal source to form jotunitic parent magmas with variable accumulations of plagioclase that intruded as suspensions into middle to upper crustal chambers, forming massive to layered anorthosites, layered intrusions, and differentiated dikes (e.g. Bolle et al. 2003; Demaiffe and Hertogen 1981; Demaiffe et al. 1986; Duchesne 1984, 1990; Longhi et al. 1999; Vander Auwera et al. 1998; Wilson et al 1996). Recently, Bogaerts et al. (2003a, 2006) undertook a detailed petrological study of one of the main intrusions of the hornblende and biotite granitoid suite, namely the Lyngdal granodiorite (Figs. 1, 2). These authors stressed its continuous trend from monzodiorite to granite and a major and trace element composition which

mimics that observed in typical rapakivi granites despite the lack of rapakivi textures. They further showed that a fractional crystallization process without significant assimilation can drive the monzodioritic parent magma toward a more evolved granitic composition. The objective of the present paper is to assess the possible petrological link between these granitoids and rare associated mafic facies. Indeed, this possible link has important implications for the way the Proterozoic continental crust differentiated. Geochemical and experimental data recently acquired on the Lyngdal granodiorite as well as published experimental data are used to establish this link. Possible sources of these mafic facies will also be briefly discussed.

Geology and geochemistry of the late Sveconorwegian hornblende and biotite bearing granitoids

The Sveconorwegian orogen of SW Scandinavia (Fig. 1) is one of the Grenvillian orogenic belt. It is interpreted as resulting from the collision between Fennoscandia (the northwestern part of the Baltic shield) and an unknown large craton at the end of the Mesoproterozoic (1130–900 Ma) (e.g. Bingen et al. 2008, 2005 and references therein). It is made of a parautochtonous segment, the Eastern segment, which mainly consists of reworked Fennoscandian crust, and of two allochtonous terranes, the Idefjorden and Telemarkia terranes. The latter one comprises several sectors (Rogaland-Vest Agder, Suldal, Hardangervidda, Telemark) which were probably part of a single piece of continent at the onset of the Sveconorwegian orogeny (Fig. 1) (Andersen et al. 2001; Bingen et al. 2005). These segment and terranes are separated by major boundary zones shown on Fig. 1. Inside the Telemarkia terrane, the Mandal-Ustaoset fault and shear zone separates the Telemark sector in the east from the other sectors to the west (Rogaland-Vest Agder, Suldal, Hardangervidda). The Bamble-Kongsberg sector is interpreted as an early-Sveconorwegian collision zone between Telemarkia and the Idefjorden terrane. The Sveconorwegian postcollisional magmatism is abundant in the Telemarkia terrane. The hornblende-biotite granitoid suite forms a plutonic belt in its center, especially voluminous on the western side of the Mandal-Ustaoset fault and shear zone (e.g. Holum, Svöfjell, Rustfjellet, Valle, Bessefjellet, Verhuskjerringi, Kleivan plutons). The actual age of intrusion of the HBG suite is estimated at around 970–950 Ma, by means of U–Pb zircon data in a few plutons: Byklom (970+14/−18 Ma, Andersen et al. 2002), Holum (957 ± 7 Ma, Bingen et al. 2006), the Lyngdal granodiorite (950 ± 5 Ma, Pasteels et al. 1979).

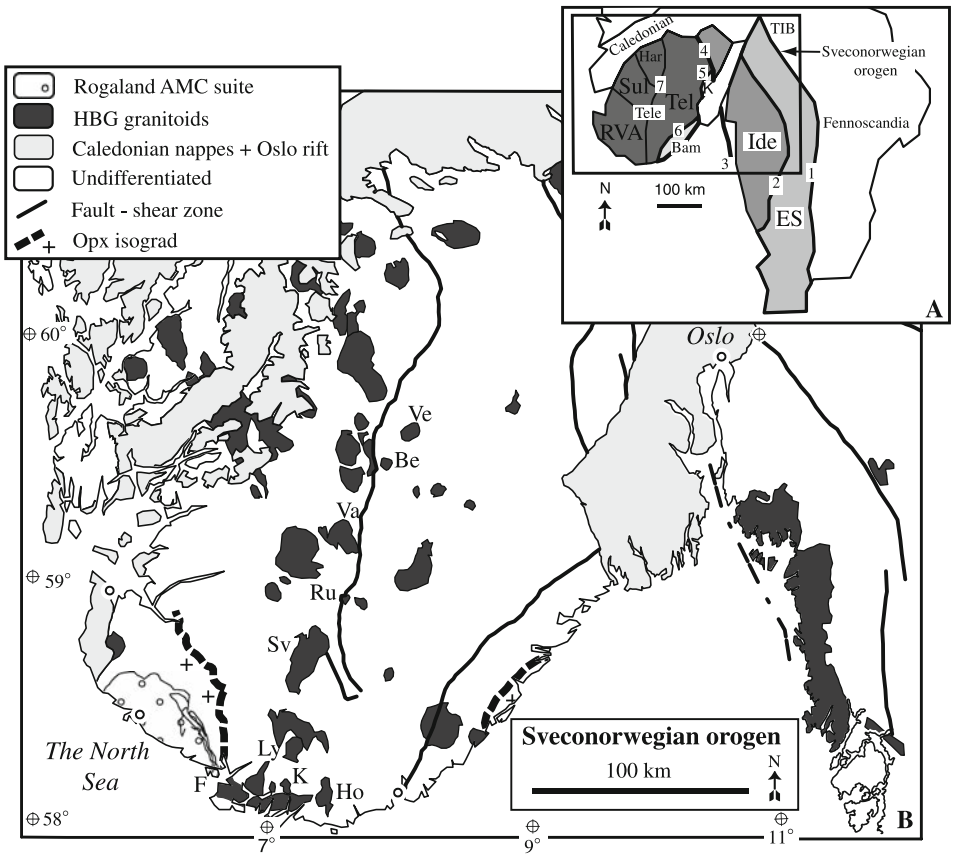

Fig. 1 **a** Situation map of SW Scandinavia and lithotectonic domains as defined by Bingen et al. (2005, 2008). *Tele* Telemarkia terrane (*RVA* Rogaland-Vest Agder; *Sul* Suldal; *Har* Hardangervidda; *Tel* Telemark; *TIB* Transcandinavian Igneous Belt), *Ide* Idefjorden terrane, *ES* eastern segment, *Bam* Bamble, *K* Kongsberg. *1* Sveconorwegian frontal deformation zone; *2* Mylonite zone; *3* Östfold-Marstrand boundary zone; *4* Åmot-Vardefjell shear zone; *5* Saggrenda-Sokna shear zone; *6* Kristiansand-Porsgrunn shear zone; *7* Mandal-Ustaoset fault and shear zone (after Bingen et al. 2005). **b** Geological sketch map of SW Scandinavia showing the Sveconorwegian postcollisional plutons. *F* Farsund, *Ly* Lyngdal, *K* Kleivan, *Ho* Holum, *Sv* Svöfjell, *Ru* Rustfjellet, *Va* Valle, *Be* Bessefjellet, *Ve* Verhuskjerringi. The Opx-in isograd related to the Sveconorwegian regional metamorphism is also shown

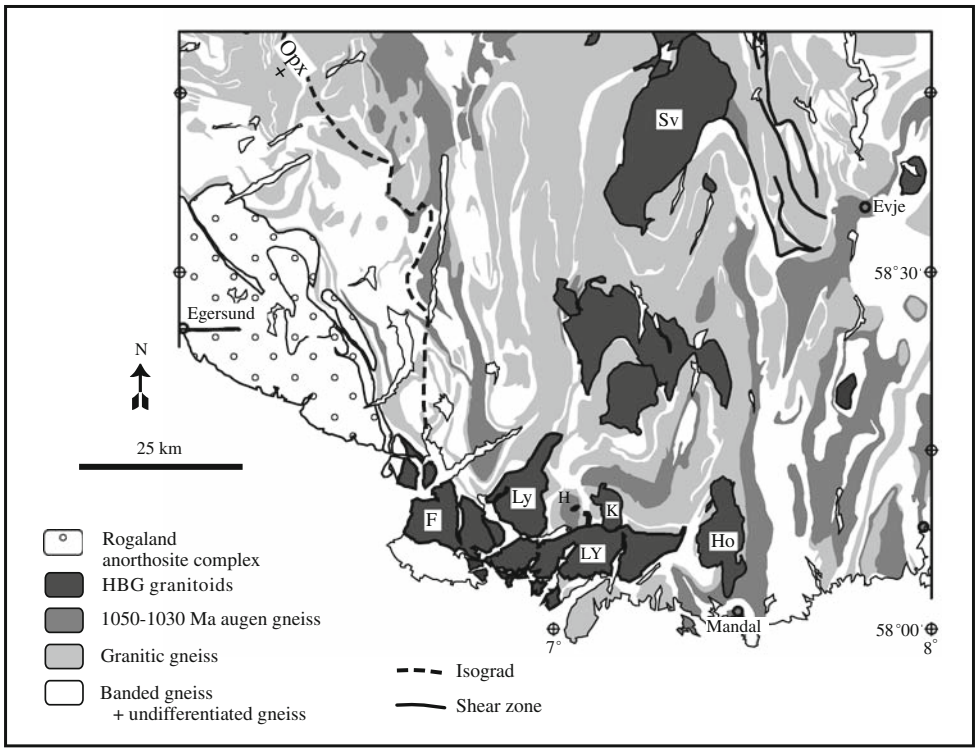

Fig. 2 Geological sketch map of southwest Rogaland showing the Rogaland Anorthosite complex and the location of the Lyngdal and Skoland gabbronorites (H) (*F* Farsund, *Ly* Lyngdal granodiorite, *Ho* Holum, *K* Kleivan) (after Bingen et al. 2006)

The Rogaland AMC suite intruded at 930 Ma in the southwesternmost part of the terrane (Fig. 1). Bingen et al. (2006) proposed that these postcollisional magmatic suites were emplaced in the Rogaland-Vest Agder sector during the two stages of doming induced by the gravitational collapse of the Sveconorwegian orogen (Andréasson and Rodhe 1994; Bingen et al. 1998, 2006; Romer 1996). This final evolution of the Sveconorwegian orogeny is defined as the Dalane phase in the four-phase model of Bingen et al. (2008).

Plutons of the hornblende–biotite granitoid suite (e.g. Holum, Svöfjell, Rustfjellet, Valle, Bessefjellet, Verhuskjerringi, Kleivan) (Fig. 1) have similar field and petrographic characteristics, and major and trace element compositions (Vander Auwera et al. 2003). Their mafic mineralogy is dominated by hornblende and biotite, in sharp contrast with the Rogaland AMC suite which is dominated by orthopyroxene. Also, these granitoids are ferroan (Frost et al. 2001), mostly metaluminous and display elevated contents in Ga and incompatible elements (A-type signature: Whalen et al. 1987). Their rapakivi-like geochemical signature has been demonstrated by Bogaerts et al. (2003a). The selected plutons define a single differentiation trend of decreasing CaO, MgO, FeO_t, TiO_2, P_2O_5 and increasing K_2O with increasing SiO_2 from 60 to 77% (Vander Auwera et al. 2003). This differentiation trend is generally lower in FeO_t/MgO and K_2O and higher in CaO and P_2O_5 than the Rogaland AMC suite. A detailed petrological and geochemical study (major and trace elements, Sr and Nd isotopes) of the Lyngdal granodiorite (Fig. 2) showed that this differentiation trend could be produced by fractional crystallization involving two successive cumulates. The first cumulate consists of clinopyroxene, plagioclase, magnetite, ilmenite and apatite with or without hornblende. The second cumulate contains the same minerals as the first cumulate with additional biotite (Bogaerts et al. 2003a). Experimental constraints further indicated that the quartz monzodioritic parent magma of the Lyngdal granodiorite was emplaced in the upper crust (0.2–0.4 GPa) as a relatively wet (5–6 wt% H_2O) and oxidized magma (oxygen fugacity at NNO to NNO + 1) (Bogaerts et al. 2006).

Additionally, Andersen (1997) and Andersen et al. (2001, 2002) undertook a comprehensive isotopic study (Sr, Nd, Pb, Hf) of the late Sveconorwegian granitoids across the Sveconorwegian orogen in order to map the distribution of isotopic reservoirs in the deep crust. Andersen et al. (2001) distinguished three groups of granitoids based on their Sr content and Sr and Nd isotopic composition: the group 1 granites (normal Sr concentration granites) have more than 150 ppm Sr, $^{87}Rb/^{86}Sr < 5$, $Sr_{i930Ma} < 0.710$ and $\varepsilon Nd < 0$; the group 2 granites have less than 150 ppm Sr, $^{87}Rb/^{86}Sr > 5$, $Sr_{i930Ma} > 0.710$ and $\varepsilon Nd < 0$; group 3 comprises one peculiar granite

characterized by low Sr_{i930Ma} (<0.710) and εNd (>0). These authors showed that granites of group 1 are the most abundant and occur all over south Norway whereas group 2 granites are restricted to north-central Telemark. The granitoids discussed by Bogaerts et al. (2003a) and Vander Auwera et al. (2003) as well as in this paper fall in the "normal Sr concentration group" defined by Andersen et al. (2001) except Bessefjell which belongs to group 2. These latter authors suggested that the isotopic compositions of these granitoids is consistent with mixing between a depleted-mantle-derived component and two components having an extended crustal history.

The late Sveconorwegian hornblende and biotite granitoids are essentially made up of intermediate (monzodioritic to quartz monzodioritic) to silicic (granitic) rocks, with rare mafic rocks. Mafic enclaves are locally reported in the Lyngdal granodiorite. Two small apparently undeformed mafic intrusions (ca. 1–2 km long) are exposed in the amphibolite-facies gneiss complex north of the Lyngdal granodiorite (Demaiffe et al. 1990). These are the Lyngdal anf Koldal "hyperites" (H on Fig. 2), hereafter referred to as the Lyngdal and Koldal gabbronorites, using valid nomenclature. The mafic facies represent a very small surface area compared to the granitoids, in agreement with what has been observed in other magmatic suites. For example, in the Chilliwack batholith of the North Cascades, Tepper et al. (1993) described mafic plutons which represent only 2% of the outcrop area. In the following, we will first discuss the geochemistry of these mafic rocks based on available compositional data and we will then examine their possible link with the granitoids.

Geochemistry of the mafic rocks

The Lyngdal and Skoland gabbronorites (Demaiffe et al. 1990) (Fig. 2) are usually medium grained (1–5 mm), homogeneous and contain plagioclase, orthopyroxene, clinopyroxene as major phases as well as minor amounts of biotite, ilmenite, magnetite, apatite, K-feldspar and quartz. A Rb–Sr isochron obtained on 10 whole rock samples plus one plagioclase separate gives an age of 910 ± 82 Ma (error at 2σ level: Demaiffe et al. 1990) which is close to the U–Pb ages obtained for the hornblende and biotite granitoid (950–970 Ma) suite. In the Lyngdal granodiorite (Bogaerts et al. 2003a), mingling between the main granodioritic magma and lobate mafic inclusions up to 50 cm wide and 1 m long has been observed locally. These will be referred to as *mafic enclaves* (samples MB2002 and VDA9912). They are fine grained (~0.5 mm) and contain hornblende, biotite, plagioclase as major phases with apatite and opaques as accessory phases. They usually contain some feldspar phenocrysts, presumably incorporated (or assimilated) from the host granodiorite.

As already noted by Bogaerts et al. (2003a), the Lyngdal and Skoland gabbronorites and the mafic enclaves display a restricted range in SiO_2 from 49.6 to 52.35% and have nearly identical compositions (Fig. 3a). The Na_2O content of the mafic enclaves (average Na_2O = 4.75%) is, however, rather high compared to that of the gabbronorites (average Na_2O = 3.70%). This could result from incorporated feldspar phenocrysts (average Na_2O = 8.4%: Bogaerts et al. 2003a) from the surrounding granodiorite into the mafic enclaves. Yet, this would translate into much higher Al_2O_3 and Sr contents in the mafic enclaves as well. As this is not observed, the higher Na_2O, and to a lesser extent K_2O, contents of the mafic enclaves are interpreted as resulting from the subsolidus mobility of alkalis. To compensate for this mobility, the Na_2O and K_2O contents of the mafic enclaves have thus been adjusted as follows. Assuming that the TiO_2 content of the mafic enclaves has not been affected by subsolidus mobility, the Na_2O and K_2O contents are calculated by multiplying their TiO_2 contents by the average Na_2O/TiO_2 and K_2O/TiO_2 ratios of the gabbronorites. Adjusted Na_2O and K_2O concentrations are shown on Fig. 3a and Table 1. Normalized to the chondrites, the spiderdiagrams of the mafic enclaves and the gabbronorites are similar and smooth with a slight negative Nb–Ta anomaly, more pronounced negative anomalies in Pb and Rb as well as a positive Ba anomaly (Fig. 3b). Available Sr and Nd isotopic data for the gabbronorites (11 samples for Sr_i and two samples for Nd, Sr_{i930Ma} = 0.70465 to 0.70544, ε_{Nd930} = +1.9 to 0.4: Demaiffe et al. 1990) and the mafic enclaves (one sample, Sr_{i930Ma} = 0.70507, ε_{Nd930} = +0.5: Bogaerts et al. 2003a) overlap one another. Thus, it appears that the mafic enclaves and the gabbronorites represent samples of the same magma as already concluded by Bogaerts et al. (2003a). The crystallization of amphibole and biotite in the mafic enclaves instead of the clinopyroxene and orthopyroxene in the gabbronorites may have been induced by migration of H_2O from the surrounding granodiorite (estimated H_2O content of 5–6%: Bogaerts et al. 2006) into the mafic enclave (estimated H_2O content 1.5%: see discussion below). Moreover, it is important to stress that mingling between the mafic enclaves and the granodiorite requires the two magmas to be contemporaneous. In Fig. 3a, primitive jotunites considered as representative samples of the parent magma of the andesine anorthosites from the nearby Rogaland anorthositic complex are shown for comparison. As already pointed out by Demaiffe et al. (1990) and Vander Auwera et al. (2003), the gabbronorites and primitive jotunites have some similarities, but also have some significant compositional differences, notably the gabbronorites have lower TiO_2 and FeO_t contents.

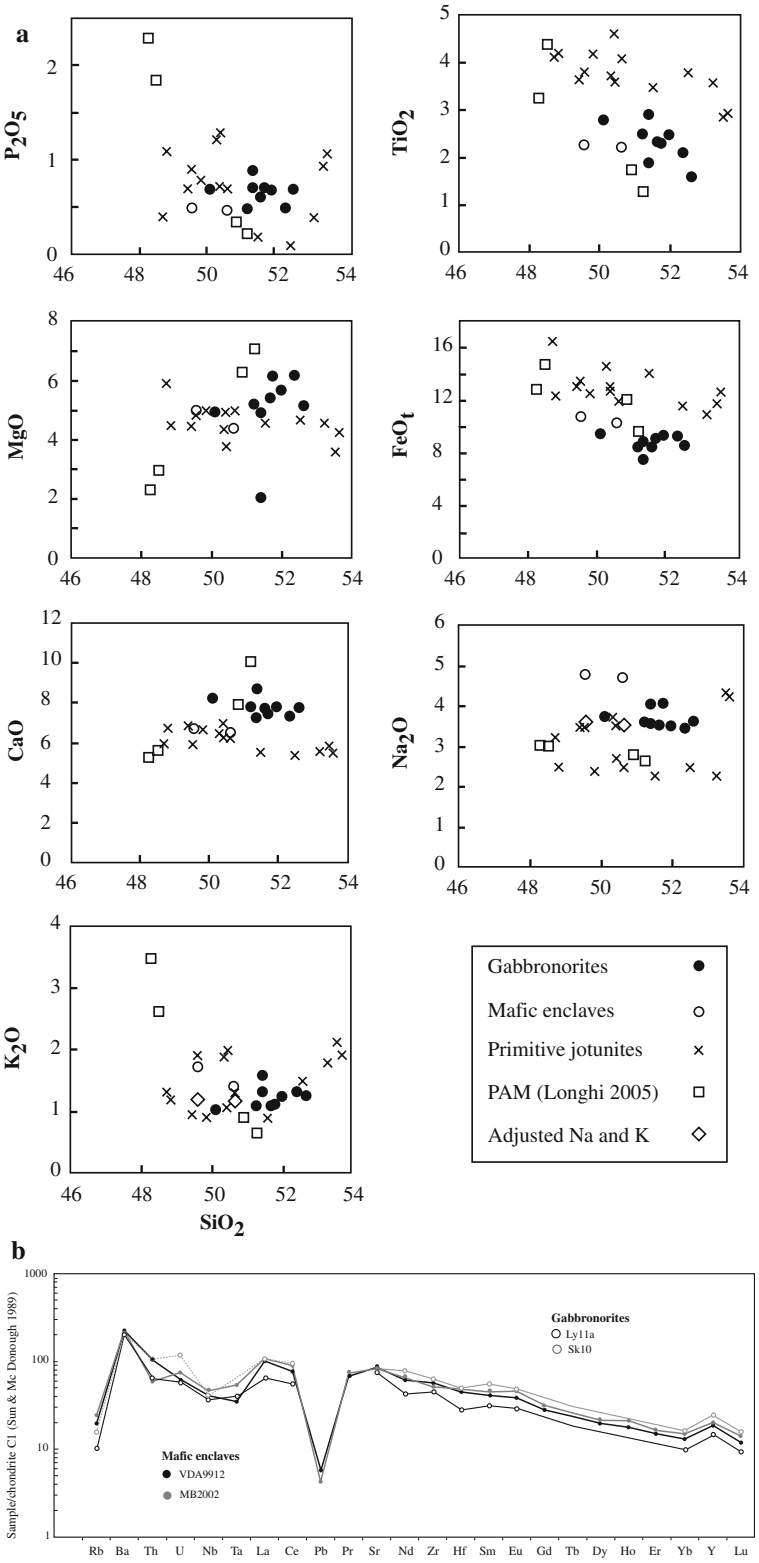

Fig. 3 **a** Major element geochemistry of the Skoland and Lyngdal gabbronorites (*filled circles*: data from Demaiffe et al. 1990) and the mafic enclaves (*open circles*: data from Bogaerts et al. 2003a). The primitive jotunites (*crosses*) of the Rogaland anorthosite complex are shown for comparison (data from Vander Auwera et al. 1998). Calculated partial melts of average post-Archean mafic crust at 1.1 GPa from Longhi (2005) (*open squares*) are also shown. Na_2O and K_2O diagrams: *open diamonds* = adjusted values for mafic enclaves (see text for explanation). **b**. Spiderdiagram comparing the trace element composition of the gabbronorites (data from Demaiffe et al. 1990) and the mafic enclaves (data from Bogaerts et al. 2003a)

Petrological link between the mafic rocks and the granitoids

The genesis of intermediate to silicic magmas is generally attributed to two main processes: differentiation from a mafic magma or partial melting of a crustal source. Additionally, crustal assimilation involving mixing with melts and crystals from various sources may also occur. Large scale mixing between mafic and silicic components to produce intermediate compositions is not retained here as

Table 1 Major and trace elements analyses of (quartz) monzodioritic compositions

Sample #	Mafic enclaves		Svöfjell					Lyngdal					
	MB2002	VDA9912	84.43	SV1	SV2	SV4	SV10	98N50	98N51	98N29	MB9918	MB9934	98N30
SiO_2	49.6	50.6	62.45	61.98	61.44	61.4	61.23	59.6	59.6	60.3	60.7	60.7	60.8
TiO_2	2.29	2.24	1.03	1.46	1.34	1.29	2.05	1.72	1.73	1.61	1.56	1.48	1.17
Al_2O_3	16.5	16.3	15.25	15.06	15.4	15.42	14.13	13.6	13.4	13.6	13.5	14.5	15.1
Fe_2O_3	12.0	11.6	3.76	3.93	4.37	4.16	4.62						
FeO			2.64	2.3	3.29	3.19	3.62						
FeO_{tot}			6.0	5.8	7.2	6.9	7.8	9.2	8.7	8.2	8.0	7.4	6.9
MgO	5.0	4.4	1.6	1.36	1.5	1.54	1.66	2.1	2.0	1.8	2.0	1.8	1.30
MnO	0.18	0.19	0.1	0.24	0.22	0.21	0.17	0.16	0.16	0.15	0.15	0.13	0.12
CaO	6.75	6.51	4.56	5.34	4.95	4.72	5.01	5.30	5.14	4.97	4.56	4.51	5.25
K_2O	1.74[a]	1.43[a]	3.84	3.38	3.62	3.72	3.79	2.85	3.07	3.10	3.60	3.83	3.21
Na_2O	4.8[a]	4.72[a]	3.19	3.15	2.43	2.8	2.85	3.1	3.1	3.2	3.4	3.2	3.2
P_2O_5	0.50	0.47	0.53	0.94	0.76	0.72	0.92	0.84	0.79	0.80	0.76	0.62	0.76
LOI	0.73	1.15						0.34	0.51	0.49	0.67	0.54	0.62
Total	100.08	99.57	98.95	99.14	99.32	99.17	100.05	98.81	98.26	98.30	98.90	98.69	98.47
Rb	57	45	125	104	117	107	110	89	98	78	118	119	96
Sr	605	610	670	719	620	641	604	525	482	465	427	464	507
Ba	537	536	1666	1384	1516	1675	1588	1510	1481	1445	1482	1713	1398
V	187	386	56	40	48	36	51	82	81	72	50	64	47
Cr	33	108	–	4.5	–	25.8	–	–	–	3.3	3.7	8	4.5
Co	38	41	–	7.3	10.2	9.2	9.4	26	22	13	13	18	11
Ni	42	41	–	–	1.6	1.0	–	3	3	3.5	13	1	–
Zr	201	217	603	535	720	734	712	525	541	546	598	485	595
Hf	5	5	16.2	14.6	21.3	22.1	22.9	19	17	–	–	–	–
Ta	0.8	0.5	–	1.5	2.2	1.6	1.9	1.9	1.7	1.2	1.8	1.5	1.2
U	0.60	0.50	2.7	3.0	3.4	2.2	2.2	1.8	1.5	1.3	1.9	1.4	1.23
Th	1.69	2.9	8.3	8.9	10.0	6.4	6.4	7.1	6.3	7.1	14.3	9.5	9.8
La	25.5	23.3	82	82	97	87	122	107	117	87	110	93	80
Ce	54	47	203	178	214	192	255	226	236	204	246	219	185
Pr	6.9	6.5	24.1	–	29.0	–	39.0	30	31	26.7	32	29	23.8
Nd	30	28	98	–	123	–	163	124	127	112	130	116	102
Sm	6.9	6.2	18.4	17.4	25.1	20.6	32.0	24.7	24.6	21.8	24.3	21.7	20.5
Eu	2.64	2.20	4.5	5.6	5.7	5.3	7.5	5.23	4.80	4.42	4.81	4.45	4.82
Gd	0.6	6	16.6	–	21.0	–	28.6	22	20	19	21	19	18
Tb	1.0	0.9	2.60	2.22	2.5	2.7	4.07	3.0	2.7	2.8	3.1	2.9	2.8

Table 1 continued

Sample #	Mafic enclaves		Svöfjell					Lyngdal					
	MB2002	VDA9912	84.43	SV1	SV2	SV4	SV10	98N50	98N51	98N29	MB9918	MB9934	98N30
Dy	5.4	5.0	14.80	–	17.90	–	22.47	16	15	15	17	16	15
Ho	1.2	1.0	3.11	–	3.70	–	4.62	3.4	3.2	3.2	3.7	3.4	3.4
Er	2.7	2.5	7.54	–	9.30	–	11.66	8.5	8.0	8.0	8.9	8.4	8.2
Tm	0.42	0.40	1.09	–	1.30	–	1.58	1.25	1.07	1.05	1.23	1.17	1.09
Yb	2.5	2.2	7.25	8	8.6	7.1	9.88	7.9	7.3	6.8	7.7	7.5	7.4
Lu	0.4	0.3	1.07	–	1.20	–	1.24	1.0	1.0	1.0	1.2	1.1	1.1
$(La/Yb)_N$	0.00	0.00	8.1	7.3	8.1	8.8	8.9	9.7	11.6	9.2	10.2	8.9	7.8
Eu/Eu*	1.13	1.09	0.75	1.01	0.75	0.80	0.74	0.67	0.63	0.63	0.62	0.64	0.73

Sample #	Lyngdal													
	MB9948	98N37	MB9940	98N12	98N32	98N43	98N42	98N49	98N54	VDA9924	VDA9925	Average	Lowest value	Highest value
SiO_2	60.9	60.9	61.0	61.4	61.5	61.6	61.8	61.8	57.6	61.2	56.3	60.7	56.34	62.45
TiO_2	1.67	1.49	1.73	1.31	1.24	1.60	1.43	1.50	2.21	1.37	1.89	1.5	1.03	2.21
Al_2O_3	13.4	12.9	12.9	15.0	14.0	14.0	15.0	13.4	12.4	13.0	14.0	14.0	12.44	15.42
Fe_2O_3														
FeO														
FeO_{tot}	8.5	8.7	8.3	7.1	7.4	8.2	7.3	7.8	11.4	7.4	9.7	7.9	5.8	11.4
MgO	1.9	1.7	1.67	1.8	1.44	1.8	1.8	1.58	2.6	1.66	2.3	1.8	1.30	2.61
MnO	0.15	0.16	0.14	0.12	0.13	0.16	0.14	0.14	0.24	0.13	0.20	0.2	0.1	0.24
CaO	5.00	4.70	4.36	4.43	4.76	4.53	4.40	4.63	5.07	4.14	5.79	4.8	4.14	5.79
K_2O	3.26	3.70	3.46	3.37	3.57	3.44	3.35	3.31	3.28	4.07	2.85	3.4	2.85	4.07
Na_2O	3.1	2.8	3.1	3.7	3.3	3.2	3.3	3.0	2.8	5.3	3.5	3.2	2.43	5.3
P_2O_5	0.83	0.82	0.74	0.53	0.74	0.72	0.57	0.67	0.94	0.65	0.88	0.8	0.53	0.94
LOI	0.35	0.79	0.72	0.48	0.46	0.72	0.53	0.78	0.33	1.15	0.87	0.6		
Total	99.04	98.78	98.15	99.17	98.47	100.01	99.63	98.58	98.91	100.14	98.30	99.01		
Rb	82	139	108	95	116	105	97	111	93	110	85	105	78	139
Sr	477	423	326	490	449	477	506	431	324	470	773	512	324	773
Ba	1554	1694	1200	1466	1247	1904	1806	1378	975	1750	1835	1530	975	1904
V	66	58	77.6	58	57	65	58	75	201	112	141	73	36	201
Cr	3	–	3	–	–	–	–	–	–	–	66	7.0	3	66
Co	24	20	15	14	18	18	22	18	28	23	18	17	7.3	28
Ni	10	3.5	–	–	–	–	5.5	1.1	10	–	2	4.5	1	13
Zr	621	779	548	600	679	652	572	570	931	756	775	640	485	931
Hf	–	18	–	18	20	16	16	23	25	22	22	19	15	25

Table 1 continued

Sample #	Lyngdal													
	MB9948	98N37	MB9940	98N12	98N32	98N43	98N42	98N49	98N54	VDA9924	VDA9925	Average	Lowest value	Highest value
Ta	1.5	1.4	1.3	1.4	1.5	1.1	1.2	2.0	2.1	1.9	1.7	1.6	1.13	2.15
U	1.5	1.3	1.10	1.22	1.03	1.4	1.6	1.8	2.3	2.3	3.6	1.9	1.03	3.6
Th	8.0	7.5	8.1	8.2	9.0	7.8	7.5	9.5	8.8	14.8	12.0	8.9	6.34	15
La	96	151	75	87	112	123	101	103	129	133	134	105	75	151
Ce	222	310	167	180	224	249	213	216	264	293	294	227	167	310
Pr	29	40	21.9	22.9	28	33	26.4	28	34	37	39	30	22	40
Nd	120	163	93	94	117	129	105	122	145	145	158	124	93	163
Sm	22.8	32	19.1	19.3	23.2	24.2	20.2	24.1	28	25.3	27	23	17	32
Eu	4.81	6.26	4.25	4.34	4.68	5.30	4.65	4.78	3.30	5.30	6.50	5.1	3.3	7.5
Gd	20	31	17	17	22	22	18	22	24	21	22	21	17	31
Tb	3.0	3.9	2.7	2.5	3.2	2.5	2.6	3.2	3.7	3.2	3.2	3.0	2.2	4.1
Dy	16	21	15	13	17	14	13	17	20	17	17	17	13	22
Ho	3.5	4.2	3.3	2.6	3.6	2.9	2.5	3.5	4.0	3.3	3.3	3.4	2.5	4.6
Er	8.6	10.7	8.2	6.9	9.3	7.1	6.6	9.3	10.6	8.7	8.5	8.6	6.6	12
Tm	1.20	1.62	1.13	0.99	1.30	1.01	1.02	1.46	1.50	1.20	1.20	1.2	1.0	1.6
Yb	7.5	10.1	7.4	6.2	8.1	6.6	6.2	8.7	8.9	7.3	6.8	7.7	6.2	10
Lu	1.1	1.3	1.1	0.9	1.2	0.9	0.9	1.3	1.3	1.0	0.9	1.1	0.9	1.3
$(La/Yb)_N$	9.2	10.7	7.2	10.1	10.0	13.2	11.8	8.6	10.4	13.0	14.2	9.8	8.7	10.7
Eu/Eu*	0.66	0.62	0.68	0.70	0.62	0.72	0.72	0.62	0.36	0.66	0.76	0.68	0.60	0.74

Eu* has been interpolated between Sm and Tb

Analyses for Svöfjell are from Vander Auwera et al. (2003), analyses for mafic enclaves and Lyngdal are from Bogaerts et al. (2003a)

[a] Adjusted Na_2O and K_2O contents: MB2002, $Na_2O = 3.63$, $K_2O = 1.21$; VDA9912, $Na_2O = 3.54$, $K_2O = 1.19$. See text for explanation

detailed geochemical and isotopic compositions obtained on another Sveconorwegian postcollisional intrusion, namely the Farsund body (Figs. 1, 2), have convincingly shown that mixing was inefficient in these magmas (Dupont et al. 2005). Thus, we will focus our attention on models of fractional crystallization and partial melting.

Fractional crystallization

In the following analysis, the mafic enclaves and gabbronorites are regarded as representing the upper crustal equivalent of sills which were mostly emplaced in the middle to lower crust probably because of an effective density filter. Locally, these mafic magmas were able to escape toward the upper crust where they mingled with the penecontemporaneous intermediate magmas. We will test the possibility that differentiation of these mafic sills at middle to lower crustal pressures can produce intermediate compositions which fall in the range of the observed least evolved compositions of the granitoids, i.e. monzodioritic compositions. Sample VDA9912 (mafic enclave) with adjusted Na_2O and K_2O has been selected as the starting composition because it is a fine-grained rock that probably closely approaches the composition of a true liquid. Table 1 and Fig. 4 display a selection of monzodioritic to quartz monzodioritic compositions sampled in the granitoids. Among these compositions, sample VDA9925 (monzodiorite) has been chosen as the final composition because it has the lowest SiO_2 content (56.3%).

By comparing natural mineral assemblages with experimental phase assemblages produced on two samples of the Lyngdal granodiorite, Bogaerts et al. (2006) showed that the quartz monzodioritic magma initially contained 5–6% H_2O. This conclusion is mainly based on the lack of orthopyroxene or pigeonite in the Lyngdal granodiorite as well as in other plutons of the HBG granitoid suite (Vander Auwera et al. 2003) and on the late appearance of biotite. It is further supported by the abundance and rather large size of pegmatites (with metric to plurimetric crystals) observed in the Lyngdal and Svöfjell intrusions (Figs. 1, 2) (Bogaerts et al. 2006). Sample VDA9925 selected as the final composition of the fractional crystallization process is slightly less differentiated (monzodioritic) than the quartz monzodioritic sample experimentally studied by Bogaerts et al. (2006). Its H_2O content should thus have been lower than that of this quartz monzodioritic composition. Using the same cumulate (cumulate 1: clinopyroxene, plagioclase, magnetite, ilmenite and apatite with or without hornblende) as Bogaerts et al. (2003a), it can be shown that 20% crystallization is necessary to drive the liquid from a monzodioritic (VDA9925) towards a quartz monzodioritic composition (98N50 of Bogaerts et al. 2006). Considering that the quartz monzodioritic magma contained 5–6% H_2O

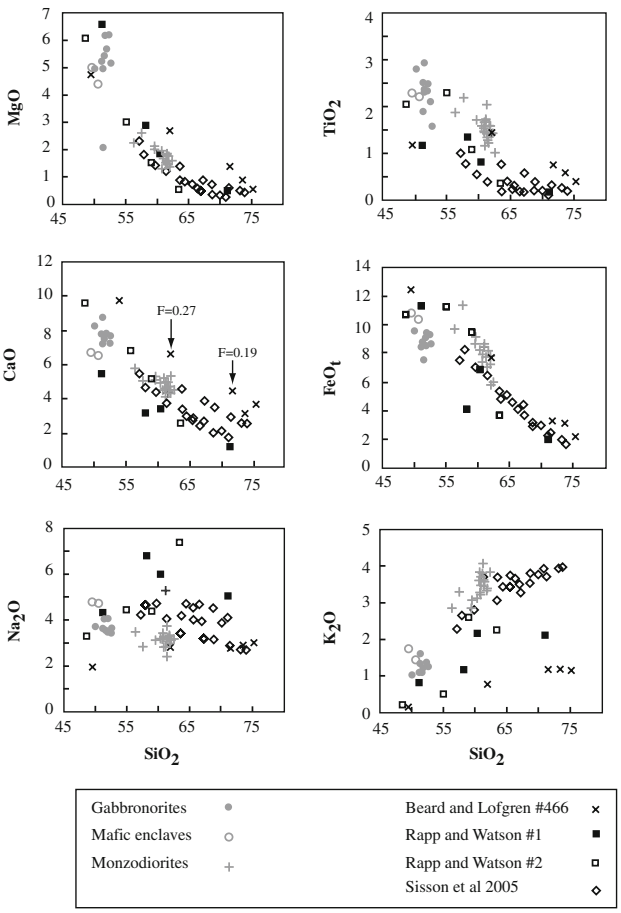

Fig. 4 Harker diagrams comparing the composition of observed (quartz) monzodiorites (data from Vander Auwera et al. 2003; Bogaerts et al. 2003a) from a selection of granitoids with experimental melts (Beard and Lofgren 1991; Rapp and Watson 1995; Sisson et al. 2005). *Arrows* indicate melt compositions for 19 and 27% melt proportion in the experiments of Beard and Lofgren (1991)

and taking into account the slight amount of H_2O included in the amphibole of the substracted cumulate, it follows that the monzodioritic magma contained 4.05–4.85% H_2O. The composition of the bulk cumulate substracted from the mafic parent magma to produce a monzodioritic residual melt has been estimated with the experimental data of Sisson et al. (2005). These authors have produced granitic-rhyolitic liquids at 0.7 GPa from moderately hydrous (1.7–2.3 wt% H_2O) basaltic compositions, which are similar to the mafic magmas considered in this study, but with lower concentrations of TiO_2 and FeO_t and higher Al_2O_3 and CaO. Their moderate H_2O contents are also adequate to produce residual melts with 4.05–4.85% H_2O. Most of the experiments of Sisson et al. (2005) were performed below 950°C in order to obtain granitic–rhyolitic liquids but a few experiments were performed at higher temperatures and are thus relevant for this study. At these temperatures and pressure amphibole is the dominant ferromagnesian

Table 2 Crystallization of the gabbronoritic composition

	Starting composition	Starting material	Final composition	Residual melt at 975°C	Mineral compositions in run 1603 of Sisson et al. (2005)				
	VDA9912	87S35A Sisson et al. (2005)	VDA9925	Run 1603 Sisson et al. (2005)	Plag	Amph	Opx	Cpx	Tmgt
SiO_2	52.8	51.3	57.8	57.4	54.71	41.90	50.97	49.31	0.22
TiO_2	2.3	1.3	1.9	0.9	0.00	3.12	0.31	0.71	11.95
Al_2O_3	17.0	19.4	14.4	17.4	28.46	13.73	4.46	6.11	7.96
FeO_t	10.9	8.8	10.0	8.9	0.71	15.08	21.08	13.04	76.33
MnO	0.2	0.2	0.2	0.2	0.00	0.25	0.62	0.45	0.44
MgO	4.6	4.4	2.3	2.1	0.00	11.75	20.67	12.94	3.10
CaO	6.8	9.0	5.9	5.0	10.30	10.61	1.72	16.61	0.00
Na_2O[a]	3.7	4.3	3.6	4.5	5.48	2.68	0.17	0.84	0.00
K_2O[a]	1.2	1.0	2.9	2.6	0.34	0.88	0.00	0.00	0.00
P_2O_5	0.5	0.4	0.9	0.9	n.a.	n.a.	n.a.	n.a.	n.a.
Mineral proportions in the cumulate (%) of run 1603 of Sisson et al. (2005)					53.43	30.14	0.55	12.33	3.56

All rock and mineral analyses recalculated to 100% after substraction of LOI and with total Fe as FeO

[a] Adjusted Na_2O and K_2O for VDA9912: see text for explanation

mineral. The mineral proportions in our cumulate were taken from their run #1603 (975°C) performed with starting composition 87S35A: 0.27 Melt (57.4% SiO_2) + 0.39 Plag + 0.22 Amp + 0.004 Opx + 0.09 Cpx + 0.03 Tmag. As shown in Table 2, this starting composition 87S35A and corresponding residual melt at 975°C are indeed very similar to sample VDA9912 (our parent magma) and sample VDA9925 (our residual melt), respectively. Some apatite has been described in the gabbronoritic samples, but it is usually associated with late biotite and granophyric pockets and is not included in early crystallizing plagioclase and pyroxenes. Moreover, apatite saturation temperatures (Harrison and Watson 1984) obtained in the mafic enclaves are rather low (MB2002: 830°C; VDA9912: 839°C) and probably below the solidus of such compositions. Apatite has thus not been included in the cumulate, in agreement with the incompatible character of REE (see below).

The Rayleigh equation and appropriate partition coefficients (Table 3) have then been used to test the fractional crystallization process with trace elements (Shaw 2006). Given that the suspected parent magmas had somewhat variable trace element compositions, four starting compositions have been used: the average trace element composition of mafic enclaves and gabbronorites, the composition of sample VDA9912, and finally the highest and lowest values for each trace element. Results are given in Table 4 and illustrated in a spiderdiagram normalized to chondrite C1 (Fig. 5). The calculated residual liquids using VDA9912 and the average composition of mafic rocks as starting compositions fit rather well the observed trace element content of the average quartz monzodioritic composition but the calculated REE contents are generally lower than the observed ones. However, given the generally good fit between observed and calculated compositions, we conclude that a fractional crystallization process cannot be rejected.

Partial melting

We will now test whether a mafic source equivalent in major and trace element composition to the gabbronorites and mafic enclaves can produce monzodioritic partial melts with the observed trace element content. In this analysis, we assume repeated emplacement of mafic sills in the middle to lower crust, the younger sills partially remelting older ones and occasionally also escaping towards the upper crust where they mingle with the monzodioritic to quartz monzodioritic liquids. Experimental data of Sisson et al. (2005) have shown that crystallization of mildly hydrous basaltic compositions at 0.7 GPa produces amphibolitic cumulates (see discussion above and also below). We will thus test partial melting of an amphibolitic source. Amphibolite dehydration melting has been experimentally studied by several authors (e.g. Beard and Lofgren 1991; Rapp and Watson 1995; Sisson et al. 2005) and comparison between a selection of these experimental melts and the Sveconorwegian monzodiorites and quartz monzodiorites is made on Fig. 4. Partial melts having a major element composition similar to the Sveconorwegian monzodiorites and quartz monzodiorites, notably with SiO_2 contents close to 60%, correspond to the highest temperatures melts (from 925°C to 1050°C). On the other hand, the K_2O and TiO_2 contents of the experimental melts are

Table 3 Partition coefficients used in modeling

	Plag	Amph	Opx	Aug	Ilm	Mgt
Rb	0.1	0.4	0.025	0.03	0	0
Sr	2.3	0.01	0.0034	0.09	0	0
Ba	0.38	0.3	0.00015	0.0023	0	0
V	0.02	2.26	1	3.1	11	60
Cr	0.03	7.53	1	2.7	16	350
Co	0.05	6.1	12	1.2	9	5
Ni	0.1	6.8	9.5	2	17	44
Zr	0	0.5	0.021	0.25	0.33	0
Hf	0.01	0.54	0.004	0.29	0.419	0.97
Ta	0.018	0.59	0.004	0.03	3.7	0
U	0.34	0.15	0.0002	0.0009	0	0
Th	0.04	0.16	0.0001	0.0015	0.09	0.025
La	0.13	0.18	0.0019	0.04	0.0023	0.006
Ce	0.11	0.37	0.0035	0.075	0.0019	0.006
Pr	0.1	0.62	0.0059	0.113	0.0016	0.006
Nd	0.09	0.86	0.013	0.15	0.0012	0.006
Sm	0.06	1.46	0.063	0.22	0.0023	0.006
Eu	0.46	1.57	0.059	0.2	0.0009	0.006
Gd	0.052	1.69	0.069	0.25	0.006	0.006
Tb	0.05	1.8	0.11	0.258	0.0095	0.006
Dy	0.048	1.91	0.15	0.267	0.013	0.006
Ho	0.046	1.79	0.2	0.275	0.022	0.006
Er	0.044	1.66	0.24	0.283	0.031	0.006
Tm	0.042	1.37	0.315	0.292	0.044	0.006
Yb	0.04	1.07	0.39	0.3	0.057	0.006
Lu	0.038	0.77	0.47	0.3	0.07	0.006

Partition coefficients for plagioclase (plag), orthopyroxene (opx), augite (aug), ilmenite (ilm) and magnetite (mgt) are those used in Vander Auwera et al. (1998). Partition coefficients for amphibole (amph) are from Sisson (1994) except for Ni (Dostal et al. 1983) and U (Villemant et al. 1981). For V, partition coefficients were taken from the following references: plag (Dunn and Sen 1994), amph (Sisson 1994), orthopyroxene (Dunn and Sen 1994), augite and ilmenite (Zack and Brumm 1998), magnetite (Duchesne, pers. comm.)

variable and partly controlled by the K_2O and TiO_2 contents of the starting compositions.

As the partial melting process involves dehydration melting of hornblende (e.g. Beard and Lofgren 1991; Rapp and Watson 1995; Sisson et al. 2005) we have used the equations formerly proposed by Hertogen and Gijbels (1976) as they take into account incongruent melting processes and the fact that some phases, here hornblende, may be used up during the melting process. These equations have now been extended by Zou (1998) and Zou and Reid (2001) to take into account the possibility of several phases melting incongruently, but in the present case only amphibole is supposed to be affected by incongruent melting and the simpler equations of Hertogen and Gijbels (1976) are thus appropriate. In the case of incongruent melting, the classical equations of Shaw (1970) cannot be used as the parameter P ($=\Sigma x_i p_i$ with p_i = fractional contribution of phase i to the melt and x_i = mass fraction of phase i in the solid) cannot be applied. It is replaced by the parameter Q which takes into account P as well as the mass fractions of the solid phases (t_i: clinopyroxene, orthopyroxene) and liquid (t_l) which are produced by the incongruent melting of hornblende (α).

$$D = \frac{D_0 - FQ}{1 - F}$$

in which

$$D_0 = \sum_i X_i^0 K_i$$

$$Q = \frac{P - p_\alpha \sum_i t_i K_i}{1 - p_\alpha (1 - t_l)}$$

$$F = \frac{L}{W_0}$$

(W_0 is the mass of the initial solid, L is mass of the liquid formed upon melting)

The proportions of the different phases contributing to the melt (p_i), the proportions of phases left in the restite (x_i) as well as the parameters (t_i, t_l) of the incongruent melting reaction of hornblende have been calculated using the experimental data of Beard and Lofgren (1991) acquired on the starting composition #466 (amphibolite) and are shown in Table 5. The starting composition #466 is indeed similar to that of sample VDA9912, except for its K_2O and CaO contents, which are significantly lower (0.15%) and higher (10.90%) than that of VDA9912 (adjusted $K_2O = 1.19\%$; $CaO = 6.51\%$), respectively. The initial modal proportions (X_i^0) of plagioclase, amphibole and Fe-Ti oxides in amphibolite # 466 are given by Beard and Lofgren (1991) and are also shown in Table 5. The non modal incongruent batch melting has been modeled in three intervals corresponding to three different batches (Table 5). The first interval corresponds to the complete incongruent melting of hornblende with a resultant melt fraction of 0.12. The melting reaction and t_i parameters have been estimated with the experimental run #38 of Beard and Lofgren (1991) (see Table 5). The second and third intervals correspond to a non-modal batch melting process and the p_i of the different phases have been estimated with runs #67 and #60 of Beard and Lofgren (1991) and correspond to a melt fraction of 0.19 and 0.27, respectively. Trace elements partition coefficients used in the modeling are given in Table 3 and results are shown on Fig. 6. For a melt fraction of 0.19–0.27, the agreement between the calculated and observed (average composition of the least differentiated compositions of the granitoids) trace element contents is very good.

Table 4 Modeling of trace elements composition with fractional crystallization

	Starting compositions					Calculated final compositions				Observed final compositions			
	VDA9912	Average	Lowest	Highest	*D*	L0 = VDA9912	L0 = Average	L0 = Lowest	L0 = Highest	VDA9925	Average	Lowest	Highest
Rb	45	31	18	57	0.18	132	91	53	167	85	105	78	139
Sr	610	567	508	639	1.24	444	412	370	465	773	512	324	773
Ba	536	432	325	537	0.29	1351	1088	819	1354	1835	1530	975	1904
V	386	–	–	–	3.22	21	–	–	–	141	73	36	201
Cr	108	–	–	–	15.08	–	–	–	–	–	7.0	3.0	66
Co	41	38	26	43	2.26	7.9	7.3	5.0	8.3	18	17	7.3	28
Ni	41	65	21	90	3.97	0.84	1.3	0.43	1.8	2.0	4.5	1.0	13
Zr	217	202	174	244	0.18	634	590	508	712	775	640	485	931
Hf	4.8	4.1	3.0	5.1	0.24	13	11	8.1	14	22	19	15	25
Ta	0.50	0.71	0.50	0.91	0.19	1.4	2.0	1.4	2.6	1.7	1.6	1.1	2.2
U	0.50	0.64	0.34	0.93	0.23	1.4	1.8	0.94	2.6	3.6	1.9	1.0	3.6
Th	2.9	2.3	1.3	3.0	0.07	9.8	7.6	4.4	10	12	8.9	6.3	15
La	23	20	16	26	0.13	73	63	49	80	134	105	75	151
Ce	47	45	34	58	0.18	136	132	99	169	294	227	167	310
Pr	6.5	–	–	–	0.25	17	–	–	–	39	30	22	40
Nd	28	27	20	36	0.33	69	65	48	88	158	124	93	163
Sm	6.2	6.2	4.8	8.4	0.50	12	12	9.3	16	27	23	17	32
Eu	2.2	2.2	1.7	2.6	0.74	3.1	3.0	2.4	3.7	6.5	5.1	3.3	7.5
Gd	6	–	–	–	0.57	10	–	–	–	22	21	17	31
Tb	0.90	0.88	0.67	1.1	0.60	1.5	1.5	1.1	1.9	3.2	3.0	2.2	4.1
Dy	5.0	–	–	–	0.64	8.1	–	–	–	17	17	13	22
Ho	1.0	–	–	–	0.60	1.7	–	–	–	3.3	3.4	2.5	4.6
Er	2.5	–	–	–	0.56	4.4	–	–	–	8.5	8.6	6.6	12
Tm	0.40	–	–	–	0.47	0.80	–	–	–	1.2	1.2	1.0	1.6
Yb	2.2	2.2	1.7	2.8	0.38	4.9	5	3.7	6.2	6.8	7.7	6.2	10
Lu	0.30	0.31	0.25	0.36	0.29	0.76	0.78	0.63	0.91	0.90	1.1	0.88	1.3

Starting compositions are from Demaiffe et al. (1990) and Bogaerts et al. (2003a). Observed final compositions are given in Table 1 (see references therein). Calculated final compositions were obtained using results from Sisson et al. (2005) (see Table 2) and the Rayleigh equation ($C_L = C0.f^{D-1}$). *D* is the bulk partition coefficient calculated with available partition coefficients (Table 3) and cumulus mineral proportions from Sisson et al. (2005) (see Table 2)

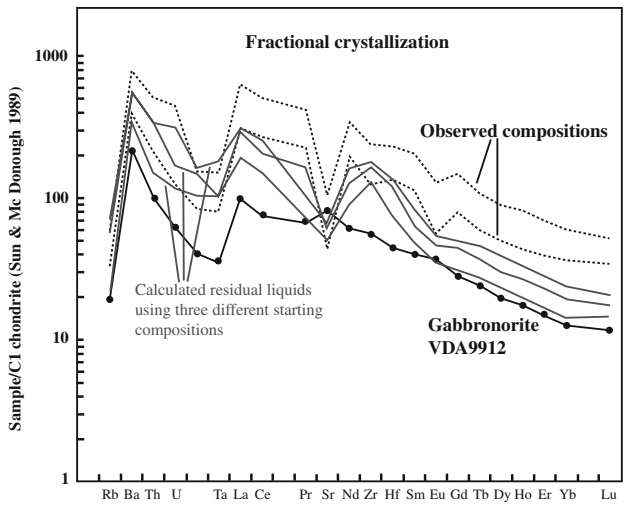

Fig. 5 Spiderdiagram comparing the composition of observed monzodioritic residual liquids (lowest and highest values) with melts calculated using a fractional crystallization process. Three starting compositions have been used: lowest values, average composition, highest values. The gabbronorite VDA9912 which has a composition very close to the average is shown for comparison. See text for explanation

Also, the major element composition of the melt corresponding to $F = 0.27$ closely matches the average major elements composition of the granitoids except for CaO and K_2O whereas for a melt fraction of 0.19, there are important discrepancies, most notably in SiO_2 (70% in the experimental melt and 60% in the average granitoids). Consequently, about 30% partial melting of an amphibolitic source produces a liquid with a major and trace element composition in agreement with the observed granitoids.

The question of H_2O

As already stated above, the H_2O content of the monzodioritic parent magma of the granitoids has been estimated to 4.05–4.85%. Given a degree of partial melting of 27% and approximating H_2O to be perfectly incompatible, it can be calculated that the amphibolite source must contain about 1.51–1.74% H_2O to produce the monzodioritic melt with such an elevated H_2O content. In amphibolites, H_2O is mainly present in amphibole. The modal proportion of amphibole in an amphibolitic source equivalent to VDA9912 is estimated by mass balance to about 40%. This value is close to the modal proportion of amphibole observed in the starting composition #466 of Beard and Lofgren (1991) (about 34%). These modal proportions enable us to estimate the minimim H_2O content of the amphibolite source to be close to 0.8% (H_2O content of amphibole = 2%). This is a minimum estimate as it does not take into account the possible availability of scarce

Table 5 Non-modal batch melting of an amphibolite

	Plag	Hornbl	Opx	Cpx	Ilm	Mgt	Liq	Rb	Sr	Ba	V	Cr	Co	Ni	Zr	Hf	Ta	U	Th	La	Ce	Pr	Nd	Sm	Eu	Gd	Tb	Dy	Ho	Er	Tm	Yb	Lu
X_0	0.56	0.34			0.014	0.087		45	610	536	386	108	41	41	217	5	0.5	0.5	2.9	23	47	6.5	28	6.2	2.2	6	0.9	5	1	2.5	0.4	2.2	0.3
Interval 1: non-modal batch melting with incongruent melting of hornblende, $F = 0.12$																																	
p_i	0.53	0.47																															
t_i			0.23	0.61			0.16	173	516	1479	64	3.0	16	7	850	14	2.0	2.0	17	93	156	17	60	9	3	9	1	8	1	4	1	3	0.4
Interval 2: non-modal batch melting, $F = 0.19$																																	
X_i	0.56		0.09	0.23	0.02	0.10																											
p_i	0.5		0.28	0.22				185	482	1467	62	3.0	24	8	892	15	2	1	14	90	184	25	107	24	5	23	3	18	4	9	1	8	1
Interval 3: non-modal batch melting, $F = 0.27$																																	
X_i	0.57		0.07	0.23	0.02	0.11																											
p_i	0.6		0.4					142	493	1253	60	3	29	8	673	12	1	1	10	70	142	19	83	18	4	18	3	15	3	7	1	6	1

Trace elements composition of the liquid produced by the non-modal batch melting of an amphibolite using the equations of Hertogen and Gijbels (1976). In the first interval, the incongruent melting of amphibole has been taken into account (Hertogen and Gijbels 1976). The initial mineralogy of the amphibolite as well as the incongruent melting reaction of the amphibole have been estimated with the experimental data of Beard and Lofgren (1991) acquired on the amphibolite #466. Partition coefficients used in the modeling are given in Table 3. The initial composition of the solid is that of sample VDA9912

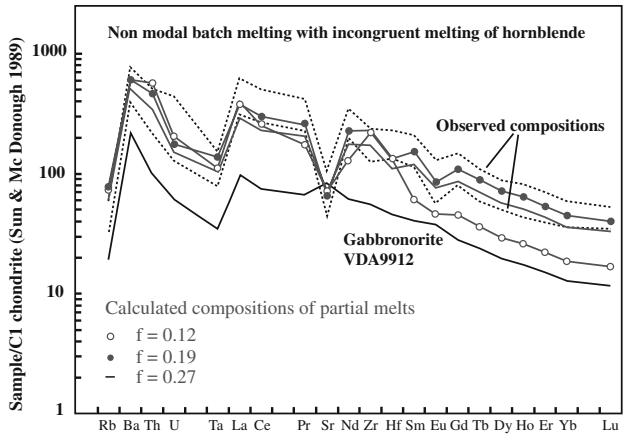

Fig. 6 Spiderdiagram comparing the composition of observed monzodioritic partial melts (lowest and highest values) with melts calculated using a non-modal batch melting with incongruent melting of hornblende. Three degrees of partial melting are shown : $F = 0.12$, 0.19, 0.27, respectively. Gabbronorite VDA9912 was used as a starting composition. See text for explanation

biotite and the H_2O present in fluid inclusions. This minimum estimate is in agreement with Annen et al. (2006). On the other hand, Rapp and Watson (1995) have estimated the total H_2O concentration of the amphibolites used as starting materials to be in the range of 0.70 to 1.65% using the LOI measured at 1,400°C. Thus, our estimate of 1.51–1.74% H_2O seems reasonable. As discussed by Bogaerts et al. (2006), the H_2O content of the monzodioritic melt at 975°C is high when compared to the negative correlation between T and H_2O^{melt} observed for a variety of granitic magmas (Scaillet et al. 1998). Clemens and Watkins (2001) explained this observed negative correlation as resulting from the buffering of H_2O^{melt} by the dehydration partial melting reactions taking place in the protoliths. However, Clemens and Watkins (2001) recognized that several high temperature natural data are more hydrous than predicted and suggested that these melts could have been produced by the breakdown of amphibole in amphibolitic source rocks for which an appropriate predictive model does not yet exist. Bogaerts et al. (2006) tentatively calculated the H_2O in melt produced during melting of amphibolite using the T-a_{H2O} solidus curve at 1 GPa proposed by Rushmer (1991) for a basaltic composition and showed that the H_2O content of the monzodioritic melt at 975°C was slightly higher than the calculated one. As mentioned by Rushmer (1991), the shape of the solidus in the T-a_{H2O} space is difficult to predict for mafic rocks. Morever, as shown above, the major element composition of the monzodiorites is not produced at the solidus of amphibolites but for rather high degrees of partial melting (30%) when amphibole reacts out. The solidus model of Rushmer (1991) is thus probably not appropriate here and based on the simple mass balance proposed above, we consider that at the present state of knowledge, the high H_2O of the monzodioritic melt can be produced by partial melting of an amphibolite.

Another question that should be adressed here is the observation that at the level of emplacement of the HBG suite, i.e. 0.2–0.4 GPa, the mafic magma crystallized as gabbronorites with a mafic mineralogy dominated by orthopyroxene and clinopyroxene, whereas in the fractional crystallization and partial melting models discussed above, we considered that in the lower crust crystallization of the same mafic magma produced mainly amphibole. For the partial melting process, we assumed that amphibolitic sources represent magmatic cumulates produced during the high pressure fractional crystallization of older sills which were later remelted by emplacement of younger ones. There are two possible solutions to solve this apparent contradiction between the pyroxene-bearing gabbronorites in the upper crust and amphibolites in the middle to lower crust. Firstly, it is possible that increasing pressure expands the stability field of amphibole in mildly hydrated mafic compositions. All experiments of Sisson et al. (2005) have been performed at 0.7 GPa and thus cannot be used here. Experimental data of Beard and Lofgren (1991) acquired at 0.1, 0.3 and 0.7 GPa on their #478 starting composition (basaltic andesite) indeed show an increasing stability field of amphibole with increasing pressure either with no added water (dehydration melting) or at water-saturated conditions. Moreover, at 0.1 GPa, the amphibole field is absent (no added water) or very restricted (water-saturated). Similarly, in the recent experimental studies of Grove et al. (2003), and Barclay and Carmicahel (2004), an important increase of the crystallization temperature of amphibole with increasing pressure has been reported and can be extrapolated to as much as 110°C for a 7 kb increase, the pressure difference between the level of emplacement of the gabbronorites and the lower crust where mafic sills crystallize to amphibolites. A second possible explanation comes from the granulitic facies conditions which prevailed during the main phase of the regional metamorphism and which produced an important volume of granulites in the westernmost part of the orogen (Figs. 1, 2). The opx-in isograd is located just west of the HBG granitoids (Figs. 1, 2) and was precisely dated at 0.97 Ga by Bingen and Stein (2003) using molybdenite produced by the dehydration melting reaction of biotite. Water produced during these metamorphic reactions could have induced the amphibolitisation of the mafic sills in the lower crust. However, even if H_2O was produced during the granulite facies metamorphism, part or all this H_2O was probably dissolved in the partial melts also produced by these reactions. Moreover, as mentioned above the mafic magmas were locally mingled in the Lyngdal granodiorite indicating that

the two magmas were contemporaneous. There were thus both emplaced at 0.95 GPa, the age of the Lyngdal granodiorite, much later than the granulite facies metamorphism. Consequently, given the present state of knowledge, we favor the first hypothesis and consider that fractional crytallization of the same mildly hydrous mafic magma produced gabbronoritic cumulates in the upper crust and amphibolitic cumulates in the lower crust.

Isotopic data

All initial isotopic ratios were calculated back to 930 Ma, the intrusion age of the Rogaland AMC suite (Charlier et al. 2007; Schärer et al. 1996) (Tables 6, 7). This permits direct comparison of isotopic data between the two magmatic suites. The monzodioritic to quartz monzodioritic compositions are represented by samples from the Svöfjell, Lyngdal, Kleivan and Holum intrusions (Fig. 2). The Sr_{i930Ma} and $^{207}Pb/^{204}Pb_{930Ma}$ of the Skoland and Lyngdal gabbronorites (Sr_{i930Ma}: 0.70465–0.70544; $^{207}Pb/^{204}Pb_{930Ma}$: 15.50–15.52: Demaiffe et al. 1990) and the monzodioritic samples (Sr_{i930Ma}: 0.70417–0.70563; $^{207}Pb/^{204}Pb_{930Ma}$: 15.44–15.48: Bogaerts et al. 2003a; Vander Auwera et al. 2003; Weis 1986) overlap within analytical errors. However, the negative εNd_{930} of the monzodiorites of −0.9 (Svöfjell, 61.2% SiO_2) to −3.14 (Holum, 63.95% SiO_2) contrast with these of the Skoland and Lyngdal gabbronorites which are characterized by positive εNd_{930} (+0.4 to +2.0). Contrarily, the initial $^{206}Pb/^{204}Pb_{930Ma}$ of the monzodiorites (16.84–17.19: Weis 1986) are lower than those of the Skoland and Lyngdal gabbronorites (17.42–17.49: Demaiffe et al. 1990). These results point to contamination by a crustal component depleted in Rb and U and enriched in LREE. Possible crustal contaminants of the postcollisional Sveconorwegian magmatism have already been discussed by Andersen et al. (2001) for the granitoid suite and Bolle et al. (2003) for the Rogaland AMC suite. These authors identified two plausible crustal endmembers. The first one (C1 in Fig. 7), proposed by Bolle et al. (2003), corresponds to the average isotopic composition of the pre-Sveconorwegian basement of southern Norway. The second one (CA of Andersen et al. 2001) equivalent to C2 of Bolle et al. (2003) (see Fig. 7) corresponds to the isotopic composition of the source region of a metacharnockite from the Bamble sector. The Sr_{i930} of crustal contaminant C1 is too high to take into account the observed isotopic compositions of the monzodiorites and quartz monzodiorites (Fig. 7). Calculations of binary mixing between a gabbronoritic composition and a crustal contaminant like C2 indicate that 20 to 40% contamination are necessary to produce the range of Sr and Nd isotopic compositions observed in the monzodiorites and quartz monzodiorites. This amount of contamination is rather high and maybe unrealistic in terms of temperature differences between the two endmembers. It partly results from the very low Sr (50 ppm) and Nd (25 pm) contents of C2 which were taken as averages of clastic metasediments from Bamble (Andersen 1997). If the average Sr (250 ppm) and Nd (83 ppm) contents of the Rustfjellet intrusion (see below) are considered for the C2 contaminant, binary mixing between the gabbronorites and C2 indicates that 10–20% contamination can reproduce the Sr and Nd isotopic composition of the monzodiorites (Fig. 7). Among the postcollisional granitoids studied by Vander Auwera et al. (2003) and Andersen et al. (2001), the Rustfjellet intrusion displays the lowest Sr_{i930Ma} (0.70274–0.70323: Vander Auwera et al. 2003) and $^{206}Pb/^{204}Pb_{930Ma}$ (15.97: Andersen et al. 2001). The Rustfjellet intrusion is a small pluton (~15 km^2) which straddles the Mandal Ustaoset shear zone (Fig. 1). It is mainly leucogranitic with elevated SiO_2 content (70.87–74.18 wt%) and an A type signature ($Ga/Al \times 10{,}000 = 3.13$–$3.70$; $Zr + Nb + Ce + Y = 281$ to 739; $FeO_t/MgO = 3.36$ to 17.10). The normative weight proportions of Qtz + Or + Ab range from 90.21 to 93.77 well above the 80% limit generally admitted to the use of the haplogranitic model (Johannes and Holtz 1996). In the Qtz–Ab–Or diagram, representative points of the Rustfjellet intrusion plot to the right of the line connecting the minimum melts compositions at different pressures. The Rustfjellet composition can thus correspond either to a minimum melt produced at around 0.7–0.8 GPa and $a_{H2O} < 0.4$ or a cotectic melt. It is also worth noting that its isotopic composition has apparently not been contaminated by the banded and granitic gneisses during emplacement in the upper crust as these gneisses have much higher Sr_{i930} (Fig. 7). On the other hand, the Rustfjellet body has negative ε_{Nd930} (−3.82) (Vander Auwera et al. 2003). Interestingly, the C2 crustal contaminant proposed by Andersen et al. (2001) and Bolle et al. (2003) has an $\varepsilon_{Nd930} = -7.8$. Calculations of binary mixing between a gabbronoritic composition and a tentative crustal contaminant were thus conducted with the latter having the Sr_{i930Ma} and initial Pb isotopic compositions of the Rustfjellet intrusion and the ε_{Nd930} of the C2 contaminant. Results indicate that 10% contamination can explain the observed isotopic composition of the monzodiorites (Table 8; Figs. 7, 8). The effect of a 10% bulk contamination on the trace elements composition of the monzodioritic melts has been tentatively assessed as follow. The trace elements composition of the contaminant has been taken as the average of samples R3, R6, R7 of the Rustfjellet intrusion (Vander Auwera et al. 2003). Sample VDA9925 has been used for the trace

Table 6 Sr, Nd isotopic data

Series name	Sample #	SiO_2 (wt %.)	Rb (ppm)	Sr (ppm)	$^{87}Rb/^{86}Sr$	$^{87}Sr/^{86}Sr$	2σ	Sr_i (930 Ma)	Sm (ppm)	Nd (ppm)	$^{147}Sm/^{144}Nd$	$^{143}Nd/^{144}Nd$	2σ	$^{143}Nd/^{144}Nd$ (930 Ma)	ε_{Nd} (930 Ma)	T_{DM} [a]
Gabbronorites	250Pl	56.9	6.1	869	0.0203	0.70565	0.00002	0.70538								
	Sk1	52.1	23	549	0.1223	0.70707	0.00002	0.70544								
	Sk2	52.4	30	508	0.1709	0.70771	0.00004	0.70544								
	Sk3a	52.0	28	527	0.1559	0.70739	0.00008	0.70532								
	Sk3b	51.7	25	639	0.1123	0.70673	0.00004	0.70524								
	Sk3b bis	51.7	25	639	0.1123	0.70670	0.00007	0.70521								
	Sk7	52.6	29	536	0.1576	0.70753	0.00006	0.70543								
	Sk9	50.1	18	565	0.0906	0.70658	0.00006	0.70537								
	Sk10	51.4	36	589	0.1769	0.70759	0.00002	0.70524	8.4	36	0.1395	0.512390	0.00002	0.51154	2.0	1337
	Ly11a	51.6	23	556	0.1207	0.70701	0.00005	0.70540	4.8	20	0.1461	0.512350	0.00004	0.51146	0.4	1556
	Ly11b	51.2	22	571	0.1135	0.70616	0.00004	0.70465								
	Ly13	51.4	30	530	0.1649	0.70730	0.00003	0.70511								
Mafic enclave	VDA9912	50.6	27	610	0.1257	0.706744	0.000011	0.70507	6.2	28	0.1320	0.512268	0.000009	0.51146	0.5	1441
Svöfjell	84.43	62.5	125	670	0.5401	0.711840	0.00004	0.70466	18	98	0.0997					
	SV10	61.2	110	604	0.5272	0.711925	0.00004	0.70492	32	163	0.1185	0.512117	0.000018	0.51139	−0.9	1482
Lyngdal	98N50	59.6	89	525	0.4908	0.711574	0.00001	0.70505	25	124	0.1204	0.512074	0.000011	0.51134	−1.9	1579
	98N29	60.3	78	465	0.4856	0.712082	0.000011	0.70563	22	112	0.1172	0.512055	0.000009	0.51134	−1.9	1556
	98N18	62.30	111	358	0.8981	0.716903	0.00001	0.70496	24.4	113.8	0.1296	0.512132		0.511341	−1.9	1646
	98N34	63.20	118	497	0.6876	0.715173	0.00001	0.70603	20.3	104.6	0.1173	0.512103	0.000008	0.511387	−1.0	1482
Tranevag	VDA9925	56.3	85	773	0.3182	0.708399	0.000011	0.70417	27	158	0.1051	0.511995	0.000009	0.51135	−1.6	1468
	VDA9926	62.50	101	524	0.5580	0.711813	0.000011	0.70440	22.5	119.6	0.1138	0.51202	0.00001	0.511326	−2.2	1556
Holum	98BN25C	63.95	108	725	0.4312	0.710394	0.000011	0.70466	28	152	0.1114	0.511957	0.000008	0.511277	−3.1	1614
Gneisses	VDA 9902	52.6	11	228	0.1425	0.710529	0.000027	0.70864	9.9	43	0.1411	0.512212	0.000008	0.51135	−1.7	1739
	VDA 9905	51.3	13	104	0.3597	0.713619	0.000014	0.70884	4.0	17	0.1434	0.512321	0.000012	0.51145	0.2	1560
	VDA 9906	73.6	13	105	0.3553	0.713082	0.00001	0.70836	7.0	33	0.1268	0.512053	0.000008	0.51128	−3.1	1732
	VDA 9907	68.5	41	119	0.9906	0.721119	0.00001	0.70795	6.7	30	0.1352	0.512222	0.000012	0.51140	−0.8	1589
	VDA 9903F	49.8	17	120	0.4026	0.723119	0.00001	0.71777	13	53	0.1444	0.512262	0.000029	0.51138	−1.1	1712
	VDA9903C	70.0	124	120	3.0196	0.773236	0.000023	0.73310	10	44	0.1211				−1.0	
	VDA9904	73.1	151	82	5.3684	0.827010	0.000013	0.75565	9.4	49	0.1161	0.512059	0.00001	0.51135	−1.7	1533

Data sources: gabbronorites (Demaiffe et al. 1990); mafic enclave, Lyngdal and Tranevag (Bogaerts et al. 2003a, b); Svöfjell, Holum and gneisses (Vander Auwera et al. 2003)

[a] Depleted Mantle model of Nelson and DePaolo (1985)

Table 7 Pb isotopic data

Series name	Sample #	$^{206}Pb/^{204}Pb$	$^{207}Pb/^{204}Pb$	$^{208}Pb/^{204}Pb$	Pb (ppm)	U (ppm)	Th (ppm)	$^{238}U/^{204}Pb$	$^{235}U/^{204}Pb$	$^{232}Th/^{204}Pb$	$^{206}Pb/^{204}Pb$ (930 Ma)	$^{207}Pb/^{204}Pb$	$^{208}Pb/^{204}Pb$
Lyngdal	0137-1/1	17.667	15.512	37.365	24	2.7	5.68	7.0142	0.051	15.247	16.58	15.44	36.65
	0134-1/1	17.658	15.511	37.357	18	1.2	5.89	4.0403	0.029	21.017	17.03	15.47	36.37
		17.668	15.521	37.401	18	1.2		4.0439	0.029		17.04	15.48	
	730420	17.580	15.496	37.451	29	1.8		3.7470	0.027		17.00	15.46	
		17.574	15.495	37.432	29	1.8		3.7456	0.027		16.99	15.45	
	771419	17.140	15.484	37.039	57	1.4		1.5564	0.011		16.90	15.47	
		17.151	15.496	37.059	57	1.4		1.5574	0.011		16.91	15.48	
	770480	17.603	15.489	37.732	20	1.4		4.2733	0.031		16.94	15.44	
	770520	17.407	15.490	37.167	31	1.2		2.3130	0.017		17.05	15.46	
		17.415	15.500	37.195	31	1.2		2.3145	0.017		17.06	15.47	
	820420A	17.145	15.500	37.021	67	1.7		1.5268	0.011		16.91	15.48	
		17.162	15.489	36.976	67	1.7		1.5259	0.011		16.93	15.47	
	880420II	17.802	15.517	37.960	21	1.6		4.7075	0.034		17.07	15.47	
	900420	17.220	15.471	37.094	49	1.6		2.0308	0.015		16.90	15.45	
	940420	17.582	15.495	37.149	23	1.1		3.0242	0.022		17.11	15.46	
Gabbronorites	10	18.649	15.605	38.197	6	0.70	3	7.9343	0.058	35.137	17.42	15.52	36.54
	11a	18.545	15.579	38.107	5	0.55	1.86	6.8248	0.049	23.849	17.49	15.50	36.98
Kleivan	91–46	17.445	15.487	36.736	47	1.7		2.1394	0.016		17.11	15.46	
	89–51	17.607	15.489	37.058	15	0.72		2.9914	0.022		17.14	15.46	
	88.5–50.5	17.156	15.471	36.787	25	0.42		1.0306	0.007		17.00	15.46	
	90–50	17.649	15.514	39.191	29	1.3		2.9601	0.021		17.19	15.48	
	90.5–46.5	17.510	15.495	37.145	60	4.2		4.2859	0.031		16.84	15.45	
FK gneiss	FK de PA66/L	17.041	15.434	36.465	39	0.13		0.2030	0.001		17.01	15.43	
gneiss	JCD78-34	18.553	15.604	37.704	15	1.7	4.05	7.1358	0.052	17.566	17.45	15.53	36.88
	JCD80-28-2	17.944	15.542	37.218	5	0.40	1.18	4.9572	0.036	15.111	17.17	15.49	36.51
	JCD73-48	17.938	15.544	36.816	30	2.6	2.5	5.3398	0.039	5.305	17.11	15.49	36.57
	JCD80-30	17.920	15.538	37.704	15	1.1	4.55	4.5732	0.033	19.547	17.21	15.49	36.78
	JCD72-111	19.832	15.694	39.760	30	7.4	55.9	16.2610	0.118	126.929	17.31	15.52	33.78

Data sources: Lyngdal, Kleivan, gneiss, Tjörn (Weis 1986); Gabbronorites (Demaiffe et al. 1990); BKSK (Barling et al. 2000)

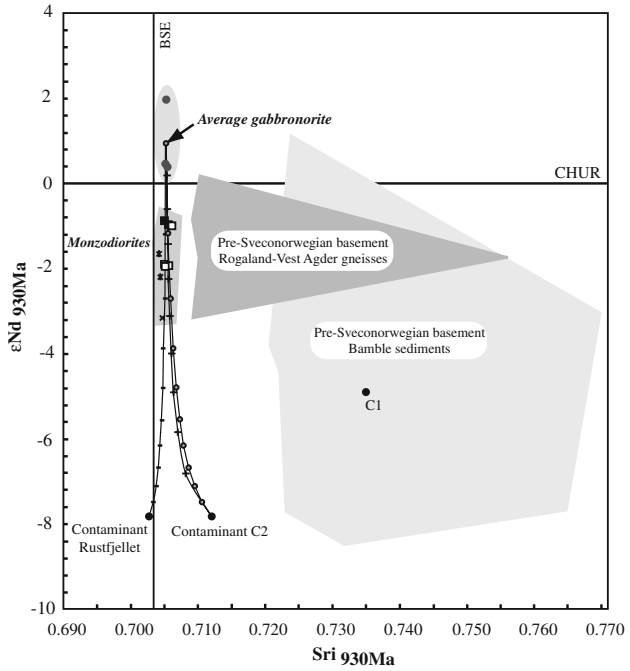

Fig. 7 $\varepsilon_{Nd930Ma}$ versus Sr_{i930Ma} for the Skoland and Lyngdal gabbronorites (data from Bogaerts et al. 2003a; Demaiffe et al. 1990) and monzodiorites (data from Bogaerts et al. 2003a; Vander Auwera et al. 2003). Data for the Rogaland-Vest Agder gneisses (Vander Auwera et al. 2003) and for the Bamble sediments (Andersen and Sundvoll 1995; Knudsen et al. 1997) are shown for comparison. C1 and C2 from Andersen et al. (2001) and Bolle et al. (2003). Mixing curves between an average gabbronorite and crustal components are broken at 10% intervals (*crosses* C2 of Andersen et al. 2001; Bolle et al. 2003); *filled circles* C2 composition modified by using Sr and Nd contents of Rustfjellet; *dashes* Rustfjellet, see Table 8). *BSE* Bulk silicate earth, *CHUR* chondritic uniform reservoir

elements composition of the monzodiorites. On Fig 9, the calculated trace element content of a monzodioritic liquid contaminated with 10 to 20% of the Rustfjellet contaminant is compared to the observed range of the monzodiorites. The effect appears negligible.

Discussion and geological implications

Available geochemical and experimental data thus suggest that both 73% fractional crystallization of a mafic parent magma and about 30% partial melting of a mafic source can produce a liquid with major and trace element composition similar to the average monzodiorites. And it is possible that both processes occurred simultaneously. As already mentioned above, mingling between the mafic and the monzodioritic components indicate penecontemporaneous magmas. Therefore, we assume that slightly older mafic rocks crystallized as amphibolites in the lower crust were then partially melted during the same geological event to produce the monzodiorites which themselves were the parent magmas of the granitoids.

Vigneresse et al. (1996) have shown that in felsic systems partial melting (solid–liquid) and crystallization (liquid–solid) are rheologically not equivalent, and have thus proposed two different thresholds for each transition. With increasing degree of partial melting, a liquid percolation threshold (LPT) is first encountered when a continuous melt film along grain boundaries connects melt pockets. For higher degrees of partial melting, a melt escape threshold (MET) allows transport of the melt and possibly part of the residue over large distances. For felsic magmas, these authors estimated that LPT and MET correspond respectively to ~8% melt and ~20–25%. During crystallization, when the proportion of crystals reaches ~55%, these crystals will interact to build a rigid structure (rigid percolation threshold, RPT) whereas at ~72–75% of crystallization, the system is locked (particle locking threshold, PLT). These rheological transitions were proposed for felsic compositions and much lower values for the melting transitions are anticipated for mafic and mantle-derived magmas (Vigneresse et al. 1996). The thresholds proposed by Vigneresse et al. (1996) thus represent upper limits when considering the genesis of the Sveconorwegian granitoids. Based on major and trace elements geochemistry, the degree of partial melting was estimated here to be around 27%. This value is in the range of the melt escape threshold (MET) proposed by Vigneresse et al. (1996). If crystallization is considered, the amount of crystallization needed to reach the appropriate monzodioritic composition (73%) is again just at the PLT proposed by Vigneresse et al. (1996). It thus appear that both processes are rheologically plausible.

Table 8 Sr, Nd and Pb systematics of crustal endmember (Rustfjellet)

	Sr (ppm)	Sr_{i930Ma}	Nd	$^{143}Nd/^{144}Nd$	$e_{Nd930Ma}$	Pb	$(^{206}Pb/^{204}Pb)_{930Ma}$	$(^{207}Pb/^{204}Pb)_{930Ma}$
Gabbronorites[a]	607	0.70525	29	0.511487	1.0	12.5	17.49	15.52
Rustfjellet[b]	250	0.70274	83	0.511039	−7.8	77	15.97	15.39

[a] Sr, Nd and Pb contents are average of samples MB2002 and VDA9912. $^{87}Sr/^{86}Sr_i$ is the average of 13 samples and ε_{Nd} corresponds to the average of 3 samples. Pb isotopic compositions are from Demaiffe et al. (1990)

[b] Isotopic data from Vander Auwera et al. (2003) and Andersen et al. (2001). Nd content is the maximum Nd content observed in Rustfjellet. Nd isotopic composition is derived from crustal pole CA and C2 of Andersen et al. (2001) and Bolle et al. (2003), respectively. See text for explanation

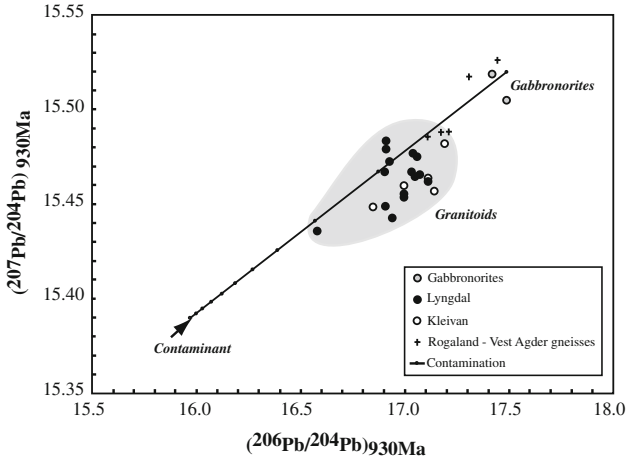

Fig. 8 Initial $^{207}Pb/^{204}Pb$ versus initial $^{206}Pb/^{204}Pb$ at 930 Ma for Skoland and Lyngdal gabbronorites (data from Demaiffe et al. 1990) and monzodiorites (data from Weis 1986) for the Lyngdal and Kleivan intrusions). Mixing curve between an average gabbronorite and a crustal component (see text for explanation) is graduated at 10% intervals

Crustal stratification

Interestingly, both fractional crystallization and partial melting produce abundant mafic rocks, either as cumulates or residues, which must be equivalent to twice the volume of the observed granitoids. As geological and geophysical evidence for large volumes of dense mafic rocks in the upper Sveconorwegian crust is lacking, we suggest that these dense mafic rocks were produced in the lower crust. The low La/Yb and Sr/Y of the HBG suite preclude any involvment of garnet in its petrogenesis. According to several experimental studies (Rapp and Watson 1995; Vielzeuf and Schmidt 2001; Wolf and Wyllie 1994), this would imply a petrogenesis at a pressure lower than about 1 GPa. However, it is worh noting that the experimental data acquired on a jotunite similar in composition to the mafic rocks discussed here (see below), garnet was only observed in the high pressure runs at 1.6 and 1.8 GPa (Vander Auwera and Longhi 1994). Formation of these granitoids thus contributed to the vertical stratification of the Proterozoic continental crust from a mafic lower to middle crust to a more felsic upper crust. The effect of crustal differentiation on trace elements can be estimated by comparing the average composition of the monzodiorites with the mafic composition (see on Fig. 5). The average monzodiorite is enriched in incompatible elements and is characterized by negative Sr and Eu anomalies as well as an enhanced Nb–Ta negative anomaly. The former can be ascribed to the important proportion of plagioclase in the cumulate or in the restite whereas the latter is either due to the significant increase in La and Ce or to the presence of ilmenite in the cumulate or restite.

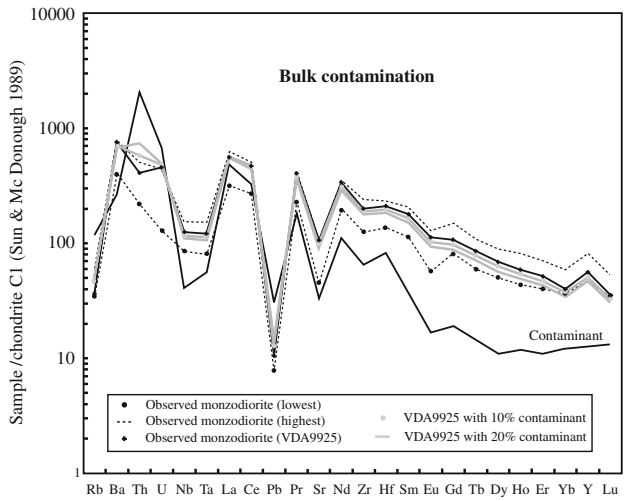

Fig. 9 Spiderdiagram comparing the composition of a monzodioritic liquid (VDA9925) contaminated with 10–20% of a Rustfjellet contaminant with the observed compositional range of the monzodiorites

Origin of the mafic component

We have already stressed that the mafic components are enriched in K_2O (1%), FeO_t (11–13%), P_2O_5 (0.5–1%) and TiO_2 (2–2.5%). This is particularly clear when comparison is made with N-MORBs (K_2O: 0.05–0.2%; FeO_t : 8.7–10.5%; P_2O_5 : 0.06–0.2%; TiO_2: 0.8–1.7%, e.g. Klein 2004). As shown on Fig. 3a, these mafic components are very similar to the so called primitive jotunites occurring in the AMC suite of Rogaland (Vander Auwera et al. 1998) and interpreted as the parent magmas of this suite. However, there are differences. Notably, the mafic rocks discussed here are lower in TiO_2, FeO_t and MnO (not shown) and slightly higher in Na_2O. When discussing the crustal versus mantle source of the AMC suites parent magmas, Longhi (2005) showed that minor element (TiO_2, K_2O, P_2O_5) concentrations of these samples cannot be reproduced by fractional crystallization with or without assimilation at 1.1 GPa for different primitive magmatic compositions and a mafic assimilant. By contrast, partial melting of a mafic lower crustal source better matches the minor elements concentrations of these mafic liquids (Longhi 2005). This can be seen in variation diagrams where calculated partial melts of average post-Archean mafic crust at 1.1 GPa are compared with the observed mafic compositions (Fig. 3a). Longhi (2005) suggested that the denser portions of lower crustal mafic/ultramafic intrusions (early and late stage cumulates) can be considered as a potential source. As the mafic rocks discussed here are very similar to the primitive jotunites, we propose here a similar model in which overdense cumulates from

lower crustal mafic/ultramafic intrusions sink back into the mantle and partially melt to produce those mafic liquids. These partial melts are then emplaced as sills in the lower crust. These mafic sills can then either be partially melted by younger mafic liquids or differentiate to produce evolved and less dense monzodioritic liquids which enables them to rise toward the upper crust. This model is schematically displayed on Fig. 10.

Amphibolite versus granulite facies source

We have already pointed out that the monzodioritic liquids, parent magmas of the upper crustal granitoids, are rather rich in H_2O (4.05–4.85%) and oxydized (NNO). As shown above, this amount of H_2O can be obtained by partially melting an amphibolitic source with a reasonable 1.5–1.7% H_2O. Direct estimation of the oxygen fugacity prevailing during partial melting of amphibolites in the middle to lower crust is not available. However, when oxygen fugacity was not externally buffered during their experiments of dehydration melting of amphibolites, Beard and Lofgren (1991) estimated the fO_2 at NNO + 1 or NNO + 2 using coexisting magnetite and ilmenite in their 0.69 GPa experiments. Partial melting of amphibolites can thus produce the appropriate monzodioritic liquids with the adequate fO_2 and H_2O content. On the other hand, if the monzodioritic liquids were derived by fractional crystallization of a mafic magma, this mafic magma should have contained a maximum of 1.7% H_2O which translates into an H_2O content of the lower crustal source between 0.34 and 0.85% for $F = 0.2$ and 0.5, respectively. Therefore, the dense cumulates of the lower crustal mafic/ultramafic intrusions must have been slightly hydrated in order to be adequate sources.

Detailed geochronological studies have defined two main phases of metamorphism in the Sveconorwegian orogeny of southern Norway (Bingen et al. 2006). The first phase dated at 1030–970 Ma is a regional Sveconorwegian metamorphism probably resulting from crustal thickening. The second phase at 930 Ma was induced by the emplacement of the Rogaland anorthositic complex and is restricted to the rocks surrounding this complex. Several lines of evidence suggest that the N–S trending Opx-in isograd formed during regional metamorphism between 1030 and 970 Ma. All plutons of the HBG suite, formed at 970–950 Ma during the waning stage of regional metamorphism, are exposed to the east of the Opx-in isograd in the amphibolite-facies domain, while all plutons of the anorthosite AMC suite formed to the west of the Opx-in isograd in the granulite-facies domain. Consequently, it is possible that the Opx-in isograd had a fundamental influence on the petrogenesis of the post-collisional magmatism. The fractional crystallization process or partial melting process described in this paper to produce the comparatively hydrated monzodioritic melt parent to the HBG suite took place in the middle to lower crust under prevailing amphibolite-facies conditions, in accordance with their position to the east of the Opx-in isograd. This is also consistent with Rudnick and Fountain (1995).

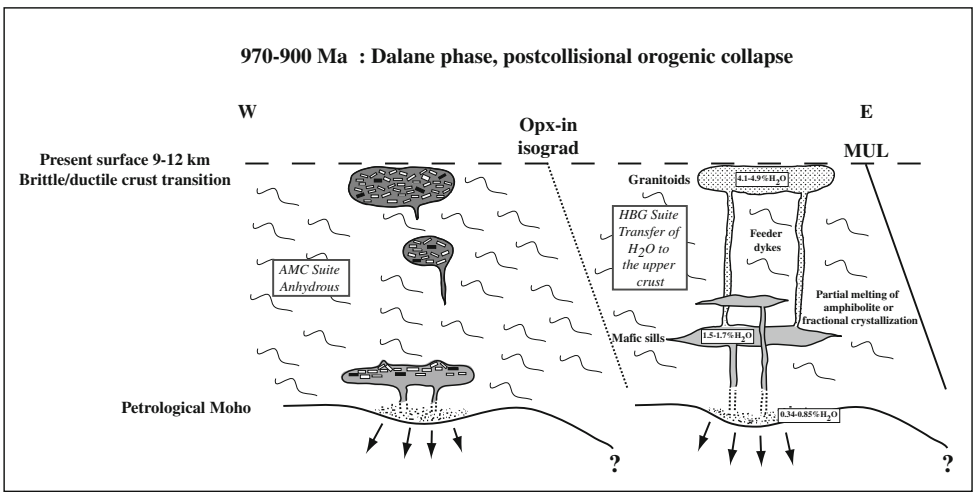

Fig. 10 Sketch showing the possible links between the monzodiorites and the mafic components together with their relative position to the Mandal-Ustaoset fault and shear zone (MUL) and the Opx-in isograd. The H_2O contents inferred for the different parts of the HBG suite are mentioned (see text for explanation). Petrogenesis of the Rogaland Anorthositic suite (AMC suite) is schematically displayed as partial melting of a lower crustal source to produce jotunitic parent magma ponded in lower crustal magma chambers where accumulation of plagioclase produces buoyant anorthositic diapirs. Moho offsets are also shown in agreement with the interpretation of deep seismic profiles by Andersson et al. (1996)

The role of fluids in the stratification of the crust

As already mentioned above, production and emplacement of the monzodioritic magmas contributed to the vertical stratification of the continental crust. Another conclusion raised by the model presented here is that during the production of these granitoids, fluid (water) was transferred and concentrated from the lower crust to the upper crust. Indeed, the lower crustal source inferred to have contained about 0.34–0.85% H_2O melted to produce mafic liquids with 1.5–1.7% H_2O. These mafic sills crystallized as amphibolites and produced monzodioritic melts with 4.05–4.85% H_2O either by fractional crystallization or by being remelted during the emplacement of younger sills. Eventually, these monzodioritic liquids were able to rise up to the surface of the Mesoproterozoic crust to produce volcanism (Bogaerts et al. 2003b) and transfer their H_2O to the atmosphere. Given an estimated volume of 600 km^3 for the Lyngdal granodiorite, a calculated density of 2,349 kg/m^3 (Bogaerts et al. 2003b) for the quartz monzodiorite and 5% H_2O, it can be estimated that the Lyngdal granodiorite contained about 70 GT of H_2O. If a volcanic edifice was indeed present above the Lyngdal magma chamber, a significant amount of H_2O was transferred from the lower crust to the atmosphere. West of the opx-in isograd, the continental crust was mostly anhydrous because in granulite facies conditions (Bingen and Stein 2003) and the AMC suite emplaced in this part of the orogen was also anhydrous. As the presence of water has a profound influence on the rheology of rocks, this difference in the water content of the crust west and east of the opx-in isograd together with the water stratification occurring east of this isograd may have played a role during the gravitational collapse of the Sveconorwegian orogen when this postcollisional magmatism was supposedly emplaced (Andréasson and Rodhe 1994; Bingen et al. 1998, 2005; Romer 1996).

Acknowledgments Technical assistance was received from G. Delhaze and J.-P. Cullus. Financial support from the FNRS (Fonds national de la Recherche Scientifique) is acknowledged. Constructive and careful reviewing by B.Bingen was greatly appreciated. A second anonymous reviewer is also thanked.

References

Andersen T (1997) Radiogenic isotope systematics of the Herefoss granite, south Norway: an indicator of Sveconorwegian (Grenvillian) crustal evolution in the Baltic Shield. Chem Geol 135:139–158

Andersen T, Andresen A, Sylvester A (2001) Nature and distribution of deep crustal reservoirs in the southwestern part of the Baltic shield: evidence from Nd, Sr and Pb isotope data on late Sveconorwegian granites. J Geol Soc 158:253–267

Andersen T, Griffin WL, Pearson NJ (2002) Crustal evolution in the SW part of the Baltic shield: the Hf isotope evidence. J Petrol 43(9):1725–1747

Andersen T, Sundvoll B (1995) Neodymium isotope systematics of the mantle beneath the Baltic shield: evidence for depleted mantle evolution since the Archaean. Lithos 35:235–243

Andersson M, Lie J, Husebye E (1996) Tectonic setting of post-orogenic granites within SW Fennoscandia based on deep seismic and gravity data. Terra Nova 8(6):558–566

Andréasson PG, Rodhe A (1994) Ductile and brittle deformation within the Protogine Zone, southern Sweden: a discussion. Geologiska Föreningens i Stockholm Förhandlinger 116:115–117

Annen C, Blundy JD, Sparks RSJ (2006) The genesis of intermediate and silicic magmas in deep crustal hot zones. J Petrol 47:505–539

Ashwal LD (1993) Anorthosites. Springer, Berlin, p 422

Barclay J, Carmicahel I (2004) A hornblende basalt from Western Mexico: water-saturated phase relations constrain a pressure-temperature window of eruptibility. J Petrol 45(3):485–506

Barling J, Weis D, Demaiffe D (2000) A Sr-, Nd-, and Pb-isotopic investigation of the transition between two megacyclic units of the Bjerkreim-Sokndal layered intrusion, south Norway. Chem Geol 165:47–65

Beard JS, Lofgren GE (1991) Dehydration melting and water-saturated melting of basaltic and andesitic greenstones and amphibolites a 1, 3, 6.9 kb. J Petrol 32(2):365–401

Bingen B, Boven A, Punzala L, Wijbrans JR, Demaiffe D (1998) $^{40}Ar/^{39}Ar$ geochronology across terrane boundaries in the Sveconorwegian Province of S. Norway. Prec Res 90:159–185

Bingen B, Nordgulen O, Viola G (2008) A four-phase model for the Sveconorwegian orogeny, SW Scandinavia. Nor J Geol 88:43–72

Bingen B, Skår Ø, Marker M, Sigmond EMO, Nordgulen Ø, Ragnhildsveit J, Mansfeld J, Tucker RD, Liégeois J-P (2005) Timing of continental building in the Sveconorwegian orogen, SW Norway. Nor J Geol 85(1&2):87–116

Bingen B, Stein H (2003) Molybdenite Re-Os dating of biotite dehydration melting in the Rogaland high-temperature granulites, S Norway. Earth Planet Sci Lett 208:181–195

Bingen B, Stein HJ, Bogaerts M, Bolle O, Mansfeld J (2006) Molybdenite Re–Os dating constrains gravitational collapse of the Sveconorwegian orogen, SW Scandinavia. Lithos 87:328–346

Bogaerts M, Scaillet B, Liégeois JP, Vander Auwera J (2003a) Petrology and geochemistry of the Lyngdal granodiorite (Souther Norway) and the role of fractional crystallization in the genesis of the Proterozoic ferro-potassic A-type granites. Prec Res 124:149–184

Bogaerts M, Scaillet B, Vander Auwera J (2003b) Emplacement of the Lyngdal granodiorite (SW Norway) at the brittle-ductile transition in a hot crust. In: Joint EGS-EUG, vol 5. Cambridge University Publications, Nice (France), p 03611

Bogaerts M, Scaillet B, Vander Auwera J (2006) Phase equilibria of the Lyngdal granodiorite (Norway): Implications for the origin of metaluminous ferroan granitoids. J Petrol 47(12):2405–2431

Bolle O, Demaiffe D, Duchesne JC (2003) Petrogenesis of jotunitic and acidic members of an AMC suite (Rogaland anorthosite province, SW Norway): a Sr and Nd isotopic assessment. Prec Res 124:185–214

Charlier B, Skår Ø, Korneliussen A, Duchesne JC, Vander Auwera J (2007) Ilmenite composition in the Tellnes deposit: fractional crystallization, postcumulus evolution and ilmenite–zircon relation. Contrib Mineral Petrol 154(2):119–134

Clemens JD, Watkins JM (2001) The fluid regime of high-temperature metamorphism during granitoid magma genesis. Contrib Mineral Petrol 140:600–606

Demaiffe D, Bingen B, Wertz P, Hertogen J (1990) Geochemistry of the Lyngdal hyperites (S.W. Norway): comparison with the monzonorites associated with the Rogaland anorthosite complex. Lithos 24:237–250

Demaiffe D, Hertogen J (1981) Rare earth element geochemistry and strontium isotopic composition of a massif-type anorthositic–charnockitic body: the Hidra massif (Rogaland, SW. Norway). Geochim Cosmichim Acta 45:1545–1561

Demaiffe D, Weis D, Michot J, Duchesne JC (1986) Isotopic constraints on the genesis of the anorthosite suite of rocks. Chem Geol 57:167–179

Dostal J, Dupuy C, Carron JP, Dekerneizon ML, Maury RC (1983) Partition coefficients of trace elements—application to volcanic rocks of St-Vincent, West-Indies. Geochim Cosmochim Acta 47(3):525–533

Duchesne JC (1984) Massif anorthosites: another partisan review. In: Brown WS (ed) Feldspars and feldspathoids, vol C137. Reidel, Doordrecht, pp 411–433

Duchesne JC (1990) Origin and evolution of monzonorites related to anorthosites. Schweiz Mineral Petrogr Mitt 70:189–198

Dunn T, Sen C (1994) Mineral/matrix partition-coefficients for orthopyroxene, plagioclase and olivine in basaltic to andesitic systems - a combined analytical and experimental study. Geochim Cosmochim Acta 58(2):717–733

Dupont A, Vander Auwera J, Paquette J-L, Pin C, Bogaerts M (2005) Inefficiency of magma mixing and source heterogeneity in the genesis of granitoids: the example of the Farsund body (southern Norway). In: Publications C (ed) Joint EGS-EUG, vol. Cambridge Publications, Nice (France), A-04915

Emslie RF (1985) Proterozoic anorthosite massifs. In: Tobi AC, Touret JLR (eds) The deep Proterozoic crust in the North Atlantic Provinces, vol C 158. NATO Adv Stud Inst, Dordrecht, pp 39–60

Frost BR, Arculus RJ, Barnes CG, Collins WJ, Ellis DJ, Frost CD (2001) A geochemical classification of granitic rock suites. J Petrol 42:2033–2048

Grove T, Elkins-Tanton L, Parman S, Chatterjee N, Müntener O, Gaetani G (2003) Fractional crystallization and mantle-melting controls on calc-alkaline differentiation trends. Contrib Mineral Petrol 145:515–533

Haapala I, Rämö OT (1992) Tectonic setting and origin of the Proterozoic rapakivi granites of southeastern Fennoscandia. Trans R Soc Edinb Earth Sci 83:165–171

Harrison TM, Watson EB (1984) The behavior of apatite during crustal anatexis: equilibrium and kinetic considerations. Geochim Cosmichim Acta 48:1467–1477

Hertogen J, Gijbels R (1976) Calculation of trace element fractionation during partial melting. Geochim Cosmichim Acta 40:313–322

Johannes W, Holtz F (1996) Petrogenesis and experimental petrology of granitic rocks. In: Wyllie PJ (ed) Minerals and rocks, vol 22. Springer, Berlin, p 335

Klein EM (2004) Geochemistry of the igneous oceanic crust. In: Holland HD, Turekian KK (eds) Treatise on geochemistry, vol 3. Elsevier, Amsterdam, pp 433–463

Knudsen T, Andersen T, Maijer C, Verschure R (1997) Trace-element characteristics and Pb isotopic evolution of metasediments and associated Proterozoic rocks from the amphibolite- to granulite-facies Bamble sector, southern Norway. Chem Geol 143:145–169

Longhi J (2005) A mantle or mafic crustal source for Proterozoic anorthosites? Lithos 83:183–198

Longhi J, Vander Auwera J, Fram M, Duchesne JC (1999) Some phase equilibrium constraints on the origin of Proterozoic (Massif) anorthosites and related rocks. J Petrol 40(2):339–362

Nelson BK, DePaolo DJ (1985) Rapid production of continental crust 1.7 to 1.9 b.y. ago: Nd isotopic evidence from the basement of the North American mid-continent. Geol Soc Am Bull 96:746–754

Pasteels P, Demaiffe D, Michot J (1979) U–Pb and Rb–Sr geochronology of the eastern part of the South Rogaland igneous complex, southern Norway. Lithos 12:199–208

Rapp RP, Watson EB (1995) Dehydration melting of metabasalt at 8–32 kbar: implications for continental growth and crust–mantle recycling. J Petrol 36(4):891–931

Romer RL (1996) Contiguous Laurentia and Baltica before Grenvillian–Sveconorwegian orogeny? Terra Nova 8:173–181

Rudnick RL, Fountain DM (1995) Nature and composition of the continental crust: a lower crustal perspective. Rev Geophys 33(3):267–309

Rushmer T (1991) Partial melting of two amphibolites: contrasting experimental results under fluid-absent conditions. Contrib Mineral Petrol 107:41–59

Rämö T, Haapala I (1995) One hundred years of rapakivi granite. Mineral Petrol 52:129–185

Scaillet B, Holtz F, Pichavant M (1998) Phase equilibrium constraints on the viscosity of silicic magmas 1. Volcanic-plutonic association. J Geophys Res B 103:27257–27266

Schärer U, Wilmart E, Duchesne J (1996) The short duration and anorogenic character of anorthosite magmatism: U–Pb dating of the Rogaland Complex, Norway. Earth Planet Sci Lett 139:335–350

Shaw DM (1970) Trace element fractionation during anatexis. Geochim Cosmochim Acta 34:237–243

Shaw DM (2006) Trace elements in magmas. Cambridge University Press, Cambridge, p 243

Sisson T (1994) Hornblende-melt trace element partitioning measured by ion microprobe. Chem Geol 117(1–4):331–344

Sisson T, Ratajeski K, Hankins W, Glazner A (2005) Voluminous granitic magmas from common basaltic sources. Contrib Mineral Petrol 148:635–661

Sun S, McDonough W (1989) Chemical and isotopic systematics of oceanic basalts: implications for mantle composition and processes. In: Saunders A, Norry M (eds) Magmatism in the ocean basins, vol 42. Blackwell Scientific Publications, Oxford, pp 313–345

Tepper JH, Nelson BK, Bergantz GW, Irving AJ (1993) Petrology of the Chilliwack batholith, North Cascades, Washington: generation of calc-alkaline granitoids by melting of mafic lower crust with variable water fugacity. Contrib Mineral Petrol 113:333–351

Vander Auwera J, Bogaerts M, Liégeois JP, Demaiffe D, Wilmart E, Bolle O, Duchesne JC (2003) Derivation of the 1.0–0.9 Ga ferropotassic A-type granitoids of southern Norway by extreme differentiation from basic magmas. Prec Res 124:107–148

Vander Auwera J, Liégeois JP, Demaiffe D, Bolle O, Bogaerts M, Duchesne JC (2001) Two distinct post-collisional magmatic suites in the Sveconorwegian of Souhern Norway: consequences for the evolution of the Proterozoic continental lithosphere. EUG XI. J Conf Abstr 6(1):769

Vander Auwera J, Longhi J (1994) Experimental study of a jotunite (hypersthene monzodiorite): constraints on the parent magma composition and crystallization conditions (P, T, fO2) of the Bjerkreim-Sokndal layered intrusion. Contrib Mineral Petrol 118:60–78

Vander Auwera J, Longhi J, Duchesne JC (1998) A liquid line of descent of the jotunite (hypersthene monzodiorite) suite. J Petrol 39:439–468

Vielzeuf D, Schmidt MW (2001) Melting relations in hydrous systems revisited: application to metapelites, metagreywackes and metabasalts. Contrib Mineral Petrol 141:251–267

Vigneresse J-L, Barbey P, Cuney M (1996) Rheological transitions during partial melting and crystallization with application to felsic magma segregation and transfer. J Petrol 37(6):1579–1600

Villemant B, Jaffrezic H, Joron JL, Treuil M (1981) Distribution coefficients of major and trace elements. Fractional crystallization in the alkali basalt series of the Chaine-Des-Puys (Massif Central, France). Geochim Cosmochim Acta 45(11):1997–2016

Weis D (1986) Genetic implications of Pb isotope geochemistry in the Rogaland anorthositic complex (southwest Norway). Chem Geol 57:181–199

Whalen JB, Currie KL, Chappell BW (1987) A-type granites: geochemical characteristics, discrimination and petrogenesis. Contrib Mineral Petrol 95:407–419

Wilson JR, Robins B, Nielsen FM, Duchesne JC, Vander Auwera J (1996) The Bjerkreim-Sokndal layered intrusion, southwest Norway. In: Cawthorn RG (ed) Layered intrusions. Elsevier, Amsterdam, pp 231–255

Wolf MB, Wyllie PJ (1994) Dehydration-melting of amphibolite at 10 kbar: effects of temperature and time. Contrib Mineral Petrol 115:369–383

Zack T, Brumm R (1998) Ilmenite/liquid partition coefficients of 26 trace elemnts determined through ilmenite/clinopyroxene partitioning in garnet pyroxene. In: Gurney JJ, Gurney JL, Pascoe MD, Richardson SH (eds) 7th International Kimberlite Conference vol. Red Roof Design, Cape Town, pp 986–988

Zou H (1998) Trace element fractionation during modal and nonmodal dynamic melting and open-system melting: a mathematical treatment. Geochim Cosmochim Acta 62(11):1937–1945

Zou H, Reid MR (2001) Quantitative modeling of trace element fractionation during incongruent dynamic melting. Geochim Cosmochim Acta 65(1):153–162